

Load Forecasting of Supermarket Refrigeration

Lisa Buth Rasmussen

DTU



Kongens Lyngby 2013
M.Sc.-2013-87

Technical University of Denmark, DTU Compute
Applied Mathematics and Computer Science
Matematik Torvet, Building 303B
DK-2800 Kongens Lyngby, Denmark
Phone +45 45253031, Fax +45 45881399
compute@compute.dtu.dk
www.compute.dtu.dk M.Sc.-2013-87

Summary (English)

The Danish power production coming from renewable energy, is increasing, therefore a flexible energy system is needed. In the present Thesis a refrigeration load forecasting method is developed, which is an important tool in a future flexible energy system.

Observed refrigeration load and local ambient temperature from a Danish supermarket, Fakta, are used. Numerical weather predictions (NWP) of ambient temperature, provided by Danish Meteorological Institute (DMI), from the model DMI-Hirlam-S05, is also used.

A multiplicative seasonal autoregressive model, only based on observations, is developed and found to be inadequate for refrigeration load forecasting. A previous developed adaptive linear time-series model is used as basic model, from that three other adaptive linear time-series models are developed. These are used for forecasting 1 to 42 hours horizon, which are evaluated and performance is compared to each other.

The models are fitted using k-step recursive least squares with forgetting, and includes regime switching, diurnal curve input and low-pass filtered ambient temperature, modelled with and without basis splines.

The achieved results clearly indicate that these methods are suitable for refrigeration load forecasting and that an enhancement of the non-linear effect from the ambient temperature in the models has occurred with spline fitted ambient temperature, seeing that the method for implementing B-splines is important for the performance of the model.

Finally ideas for further refinements, such as other local inputs i.e. relative humidity in the Supermarket are discussed. Future use of the method such as controlling load consumption from a single cabinet or from several Supermarkets are also discussed.

- Keywords: refrigeration load, prediction, recursive least squares, B-splines

Resumé (Danish)

Den danske el produktion der kommer fra vedvarende energi øger kraftigt, behovet for et fleksibelt energisystem er derved større end nogensinde før. I denne rapport udvikles en model der kan forudsige køle/fryseboksers elforbrug, hvilket kommer til at være et vigtigt redskab i det fremtidige fleksible energisystem.

Målt elforbrug fra køle/frysebokse og lokal målt udetemperatur fra det danske supermarked Fakta, bliver brugt sammen med forudsigelser af udetemperaturen fra modellen DMI-Hirlam-S05 leveret af Dansk Meteorologisk Institut (DMI).

Der er udviklet en multiplikativ autoregressiv model med sæson korrigering, hvilket kun inkluderer observationer og er fundet utilstrækkelig til brug for forudsigelse af køle/fryseboksers elforbrug. En tidligere udviklet adaptiv lineære model bliver brugt som referencemodel, hvorfra tre andre adaptive lineære modeller er blevet udviklet. Disse modeller bliver brugt til at udregne forudsigelser der består af timeværdier op til 42 timer frem i tiden, som derefter evalueres og sammenlignes med hinanden.

Modellerne er modelleret med k-step rekursive mindste kvadraters metode med glemsel og indeholder regime skifte, input fra døgn kurve og lav-pas filtreret udetemperatur, både med og uden brug af basis splines.

De opnåede resultater indikerer tydeligt, at metoderne der er brugt i disse modeller er velegnet til forudsigelse af elforbrug fra køle/frysebokse i et supermarked. Den ikke-lineære effekt fra udetemperaturen er forklaret bedre i modellerne med lav-pas filtreret udetemperaturer modelleret med basis splines, hvorfor det bemærkes at metoden for implementeringen af basis splines er vigtig for en god

præstation.

Afslutningsvis bidrager rapporten med en diskussion af idéer til forbedring, såsom andre lokale målinger som input, f.eks. den relative fugtighed i supermarkedet. Fremtidig brug af metoden, til f.eks. styring af elforbrug for en enkelt køledisk eller for flere supermarkeder, er også diskuteret.

Preface

This thesis was prepared at the department of Applied Mathematics and Computer Science at the Technical University of Denmark, in partial fulfilment of the requirements for acquiring an M.Sc. in Mathematical Modelling and Computing, written under supervision of Peder Bacher and Henrik Madsen, from February 2013 to August 2013 and accounts for 30 ECTS.

The thesis deals with modelling of load forecasting for supermarket refrigeration, with use of local ambient temperature and numerical predicted ambient temperature.

The thesis is written in English.

Lyngby, 11 August. 2013

Lisa Buth Rasmussen

Acknowledgements

I would like to thank my supervisors, Peder Bacher and Henrik Madsen for guidance throughout this thesis. And especially a great thanks to Peder, for all his help and for being available when needed for technical support.

Thanks to Christian Heerup from Danish Technological Institute, Torben Green and Kristian Fredslund from Danfoss for providing data and essential knowledge.

At last I would like to thank my friends and family, for their enormous support and understanding.

Abbreviations & Symbols

Abbreviations

ACF	Autocorrelation function , page 20
ANN	Artificial Neural Network , page 2
ARIMA	Autoregressive Integrated Moving Average , page 17
CTSM	Continuous Time Stochastic Modelling , page 87
DMI	Danish Meteorological Institute , page 8
ML method	Maximum Likelihood method , page 19
MLE	Maximum Likelihood Estimators , page 22
NWP	Numerical Weather Prediction , page 8
PACF	Partial Autocorrelation function , page 20
RLS	Recursive Least Squares , page 38
RMSE	Root Mean Square Error, page 11

Symbols

α_a	Stationary gain from ambient temperature , see equation (4.1), page 38
α_j	Spline coefficients , see equation (4.7), page 40

α_{diu}	Coefficient vector for the harmonics , see equation (4.6), page 39
θ	Parameter vector , see equation (3.5), page 22
θ_i	Estimated parameter i , see equation (3.10), page 23
Δt	Age of the data in hours , see equation (4.4), page 39
$\delta(t_{tod}, n_{har}, \alpha_{diu})$	Diurnal curve , see equation (4.6), page 39
ϵ_{t+k}	Error for horizon k , page 11
$\hat{\sigma}_\epsilon^2$	Estimated variance of the error , see equation (3.5), page 22
λ	Forgetting factor for the RLS algorithm, see Definition 4.1 , page 39
$\log L(\mathbf{Y}_N; \theta; \hat{\sigma}_\epsilon^2)$	Loglikelihood function , see equation (3.5), page 22
\mathbf{X}_t	Regressor vector , see equation (4.4), page 39
\mathbf{Y}_N	All observations , see equation (3.5), page 22
\mathbf{z}	Knot sequence , page 40
∇^d, ∇_s^D	Difference operator, s-seasonal difference operator , see equation (3.1), page 18
ω_{jp}	Weights for B-spline , see equation (4.11), page 41
ϕ_{kk}	Partial autocorrelation function , see equation (3.3), page 20
$\rho_{XX}(t_1, t_2)$	Autocorrelation function , see equation (3.2), page 20
σ^2	Variance , see equation (3.2), page 20
$a_{T_a} \in [0, 1]$	Parameter for low-pass filter , see equation (4.2), page 38
B	Backward shift operator , see equation (3.1), page 18
$B_{j,1}$	First-order B-spline , see equation (4.8), page 41
$B_{j,p,\mathbf{z}}, B_{j,p}$	j^{th} B-spline of order p and knot sequence \mathbf{z} , see equation (4.7), page 40
b_{jp}	Polynomials of order p , see equation (4.13), page 42
c	Constant , see equation (3.5), page 22
$F_{0.05}(1, f)$	F-distribution with f degrees of freedom and 0.05 significant level , see equation (3.11), page 23

$H_a(q)$	Low-pass filter , see equation (4.1), page 38
N	Number of observations , page 7
n_{har}	Number of harmonics , see equation (4.6), page 39
p	Order of splines , see equation (4.7), page 40
q^{-1}	Backward shift operator , see equation (4.2), page 38
Q_t	Observed refrigeration load at time t , page 7
Q_t^T	Transformed refrigeration load at t , page 24
$S_{p,\mathbf{z}}$	Spline function with order p and knot sequence \mathbf{z} , see equation (4.7), page 40
$T_t^{a,obs}$	Observed ambient temperature at time t , page 7
t_{tod}	Time of day in hours at time t , see equation (4.6), page 39
$w(\Delta t)$	Weights for the RLS algorithm , see equation (4.4), page 39
i,j	Indexes
k	Horizon index
t	Time index

Contents

Summary (English)	i
Resumé (Danish)	iii
Preface	v
Acknowledgements	vii
Abbreviations & Symbols	xi
1 Introduction	1
1.1 Previous Studies	2
1.2 Thesis outline	3
2 Data	5
2.1 Data from a Supermarket	5
2.2 Numerical weather prediction data	8
2.3 Preprocessing and Combining local observations with forecasts	9
2.4 Replacements of missing data	13
2.5 Exploratory analysis	15
3 Autoregressive Integrated Moving Average model	17
3.1 Methods	19
3.1.1 Autocorrelation function and partial autocorrelation function	20
3.1.2 Box-Cox transformation	20
3.1.3 Parameter estimation method	22
3.1.4 Test for lower order model	23
3.2 Model identification, estimation and evaluation	23

3.3	Model performance	35
4	Adaptive Linear Model	37
4.1	Methods	37
4.1.1	First order low-pass filtering	38
4.1.2	Recursive Least Squares with forgetting	38
4.1.3	Diurnal curve	39
4.1.4	Basis splines	40
4.1.5	Parameter optimization	43
4.2	Basic Model	44
4.2.1	Previous tests	45
4.2.2	Model evaluation	45
4.3	Basic model with regime from diurnal curve	55
4.3.1	Model evaluation	56
4.4	Basic model with splines in off-line setting	63
4.4.1	Model evaluation	66
4.5	Basic model with splines in on-line setting	72
4.5.1	Model evaluation	74
5	Results	79
6	Discussion	83
6.1	Future work	88
7	Conclusion	89
	List of Figures	93
	List of Tables	99
	Bibliography	101

Introduction

Nowadays there is an increased focus on the studies concerning the integration of renewable energy sources into existing energy systems. In 2025 it is a goal that 50% of Denmark's electricity is coming from wind power, thus a project of developing a Smart Grid is running in Denmark. This project is going to ensure greatest coherence between production and energy consumption, on the basis of this, a platform called iPower is created, which is a collaboration of 32 partners, universities and research institutions as well as industrial companies from various countries.

The idea of iPower is to develop an intelligent and flexible energy system that can handle a fluctuating power generation. This increased flexibility in power consumption enables a consumption that follows the generation of wind power and thus less needs for investment in electric energy distribution. The primary focus is to develop methods and tools for intelligent control of decentralized power consumption and production, to manage millions of flexible consumption units.

One of the challenges for developing the flexible energy system, is to create application-configurable control schemes for the industrial consumption side. The ability for the power consumers to contribute with flexibility is key factor in developing this Smart Grid. An industrial consumer, that could be flexible is the Danish supermarkets, they are using a large amount of electricity on lighting, cashiers, refrigerators and coolers etc.

The aim of this thesis is to improve the forecast model build in Bacher et al. (2013), which is able to forecast the load by the refrigerators, display cabinets and freezers in a supermarket, for short horizons. The purpose of this model is to be used for a controlling device, which main purpose is to regulate the load consumption from refrigeration by adjusting the temperature in the coolers, to a period with low prices, for money saving and to make use of the renewable energy sources.

To narrow down data complexity, only a short summer period is selected for modelling in this thesis. Initially a simple linear model solely based on past observations, will be investigated. Then the adaptive linear time-series model from Bacher et al. (2013) is recreated with the selected data and after that a different approach for regime splitting is investigated and the input from the ambient temperature is implemented with spline functions in two steps; first step with use of the observations in an off-line setting and second step in a recursive on-line setting. Each model performance is evaluated for 1 to 42 hours horizons, considering power trading at Nordpool. In the end they are compared to each other and further improvements are discussed.

1.1 Previous Studies

Before even starting the studies in this thesis, previous studies are investigated, to see if any useful informations can be obtained. After a significant amount of time spent on searching for previous studies, with a forecast model for same purpose, only one similar was found, besides from Bacher et al. (2013), which will be described later in the thesis.

- An application of neural networks for predicting energy consumption in a supermarket. An Artificial Neural Network model (ANN) with different independent input variables was developed at Brunel University (Datta et al.). The results are presented and also compared to the more traditional multiple regression techniques. This model is made for predicting the overall power consumption of the super market, every half hour. The ANN model is compared with a multiple linear regression model and a multiple polynomial regression model. This paper concludes that the ANN-model is better than any of the other, which is compared with a correlation coefficient, that measures how well the predictions agree with a target.

An ANN-model is known as a black-box model, where a system can be viewed in terms of input and output, without any knowledge of the internal work and without any opportunity for inspecting the inner components. The disadvantage for ANN-models is that they need training, that requires large number of input patterns, from e.g. observations. The model investigated in this thesis is able to make a prediction with only a small amount of observation data and primarily information from predicted weather inputs.

1.2 Thesis outline

The Thesis is describing and presenting the forecast models progressively and the report should therefore be read in succession. The following is a short presentation of each chapter.

Chapter 2 - Data The data used in the thesis is presented. An exploratory analysis is carried out, together with the preprocessing of the data before it is used for the analysis.

Chapter 3 - Autoregressive Integrated Moving Average model A forecast model which only uses observed refrigeration load, is developed. First the methods used is presented and then the model is developed stepwise with use of residual analysis. The forecast performance is evaluated.

Chapter 4 - Adaptive Linear Model First an already existing forecast model is described, evaluated and used as basis model. Then three other forecast models is developed from the basis model and evaluated.

Chapter 5 - Results The forecast performance of the identified model in Chapter 3 and each model in Chapter 4 are compared to each other and evaluated.

Chapter 6 - Discussion The results and the possibilities of improving the results through further studies, are discussed.

Chapter 7 - Conclusion Summarizes and concludes on the discoveries in the thesis.

The thesis is containing an extensively amount of illustrations and plots, so the reader might find the lists of figures and tables useful as tools for navigation, it is located after the bibliography. A lot of notation is used and the reader may need to return to the list of abbreviations and symbols, given before Table of Contents.

In this chapter the data used in the thesis, is presented and the applied pre-processing is described. Data quality has a significant influence on the modelling results, therefore the data needs to be investigated and processed to have the best possible foundation for building a good forecast model.

The measuring of load and ambient temperature were conducted in EUDP-I ESO2 project, see (Fredslund, 2013) for a detailed description and is presented in Section 2.1. The weather prediction data are provided by the Danish Meteorological Institute (DMI) and is presented in Section 2.2. A pre-processing of the data is carried out in Section 2.3 and Section 2.4 and at last a small exploratory analysis is conducted in Section 2.5.

2.1 Data from a Supermarket

The data is acquired from a Danish supermarket, Fakta, located in Otterup, Fyn. Fakta has opening hours from 8 to 21 and consists of the measured load from two types of display cabinets (low temperature and medium temperature) and also the ambient temperature T_a . The low temperature and the medium temperature consists of several different cabinets, which are listed in Table 2.1 and Table 2.2.

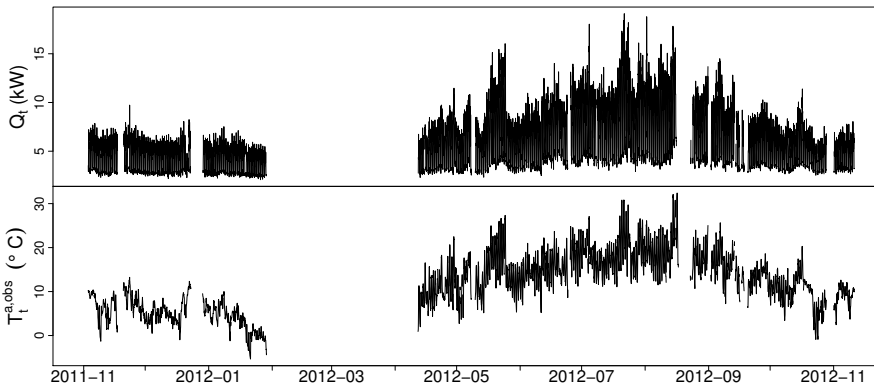
Table 2.1: List of low temperature cabinets.

Type	Model	Power (kW)
Frozen basin with glass lid	Malmoe 3	1.05
Frozen basin with glass lid	Malmoe 3	1.05
Frozen basin with glass lid	Malmoe 3	0.68
Frozen storage	ECO STE 32BL7 ED	4.80

Table 2.2: List of medium temperature cabinets.

Type	Model	Power (kW)
Milk cooling room	ECO MTE 25L7	1.05
Milk cooling room	ECO STE 32BL7	1.05
Cooling rack	Lisbona	0.68
Cooling rack	Lisbona	4.80
Cooling rack	Lisbona	5.77
Vegetable cooler	Lisbona	4.60
Cool basin with glass lid	Malmoe 3	1.27

The refrigeration load is the sum of all these cabinets and the period acquired are from November 7th 2011 to November 15th 2012. The load and the ambient temperature are measured every minute, which is re-sampled to hourly values as average values and the time stamp for average values are set to end of the hour, i.e. the load from time 04:00 to 05:00, has the time stamp 05:00. A time series plot of all the observations are displayed in Figure 2.1.

**Figure 2.1:** Top plot is the refrigeration load and bottom plot is the measured ambient temperature of all observations.

For many days the data is unavailable, there is a large gap in week 6 to 15,

which is due to a downtime for the logging computer (Fredslund, 2013). The main reasons for other gaps, large or small are; computer issues, Windows update or rebooting.

The quality of the data acquired from the supermarket, is a major subject with concern to all the missing data and the gaps. It is desirable to have a period of data, where there are not too large amounts of data unavailable. A summer period from May 1st to August 1st 2012, is selected for further processing and modelling. The refrigeration load is higher in the summer period than in the winter and is exposed to higher variations in the climate conditions. Therefore it is found reasonable to focus on a summer period.

The hourly data is in kW and denoted by

$$\{Q_t, \quad t = 1, \dots, N\}$$

and the observed ambient temperature is in °C and denoted by

$$\{T_t^{a,obs}, \quad t = 1, \dots, N\}$$

where $N = 2208$.

A plot of the selected period is displayed in Figure 2.2.

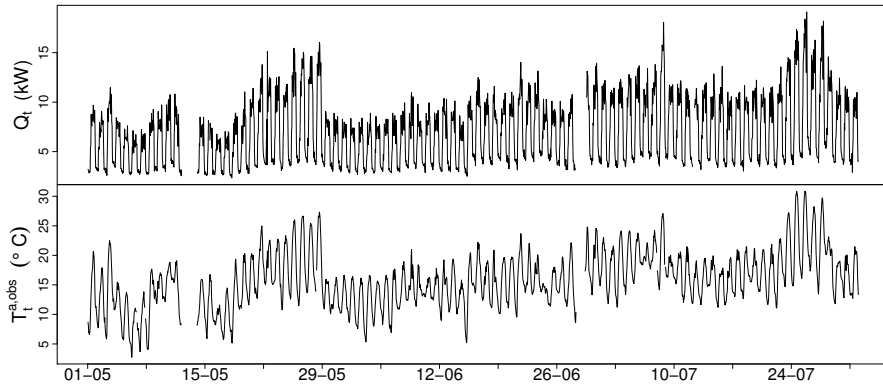


Figure 2.2: Time series plot of the hourly measurements for the selected period, load is the top plot and ambient temperature is the bottom plot.

It is clear to see, that the system has two regimes; nighttime and daytime, where at night the load is lower than daytime. This is mainly because the supermarket is closed at night, and the open cabinets are covered by isolation material. Also,

some regular peaks can be found, often in the beginning of opening hours, which are related to defrosting of the low temperature cabinets, example seen in Figure 2.3.

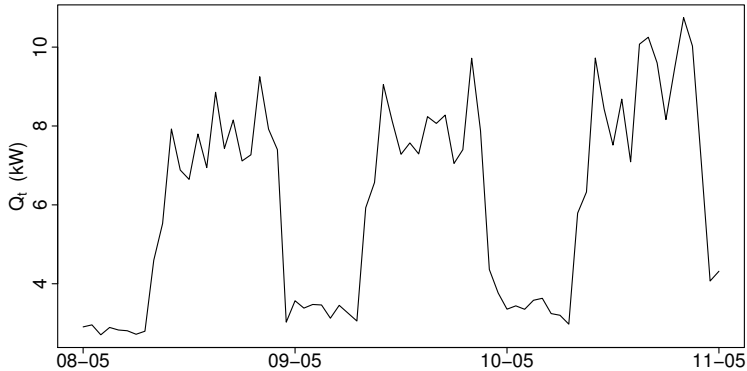


Figure 2.3: Time series plot of the hourly measurements for three selected days, for displaying the daily curve.

This defrosting is scheduled individually for the different type of coolers and cabinets, at the same time each day, two times a day, in the morning and evening, except for the weekend where the evening defrost occurs two hours earlier. For more detailed information about the system, see (Fredslund, 2013).

It is worth noticing that when ambient temperature increase, then the load at nighttime and the load in the daytime increases, partly due to the outside placement of the compressor. The daytime load increases more than the nighttime load, since the air temperature in the supermarket varies more in opening hours, and has a larger effect, due to people opening the cabinets.

2.2 Numerical weather prediction data

The numerical weather predictions (NWP) used in the models are provided by Danish Meteorological Institute (DMI). The model used by DMI, to make these NWPs, is DMI-HIRLAM-S05, which has a 5 kilometers grid and 40 vertical layers, see homepage (DMI). The NWPs consist of climate variables, with hourly values, which are updated four times per day and takes 4 hours to complete, i.e. the forecast starting at 06:00 is available at 10:00.

The predicted ambient temperature is in °C and the k^{th} horizon is denoted by

$$\left\{ T_{t+k|t}^{a,nwp}, \quad t = 1, \dots, N, \quad k = 1, \dots, 42 \right\} \quad (2.1)$$

where $N = 2208$.

In this thesis the climate variable, ambient temperature, will be used where horizon $k = 1$ to $k = 42$ is available. The NWP's are received in UTC-time and the observed temperatures are in UTC+1 time (plus 1 hour in summertime), so to get them in the same time, the NWP's are lagged by 2 hours, see Figure 2.4, where it is clearly seen that the values fit better when lagged.

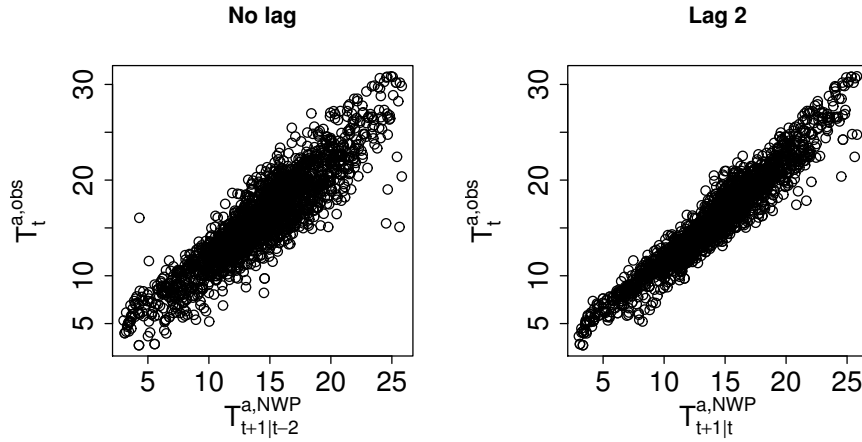


Figure 2.4: Scatterplots of the observed ambient temperature versus NWP's, to the left is with the NWP's in UTC-time and observed in local time, to the right the NWP's are lagged to local time.

2.3 Preprocessing and Combining local observations with forecasts

Due to the fact that the predicted ambient temperature $T_{t+k|t}^{a,nwp}$ is a "global" temperature for the area where the supermarket is located and the observed ambient temperature is local, mounted under the compressor, they need to be adjusted to fit each other. It is clearly seen in Figure 2.5, that the predicted

ambient temperature has a tendency to always predict a lower temperature, approximately between 1 to 5 °C, than the observed temperature for the same hour.

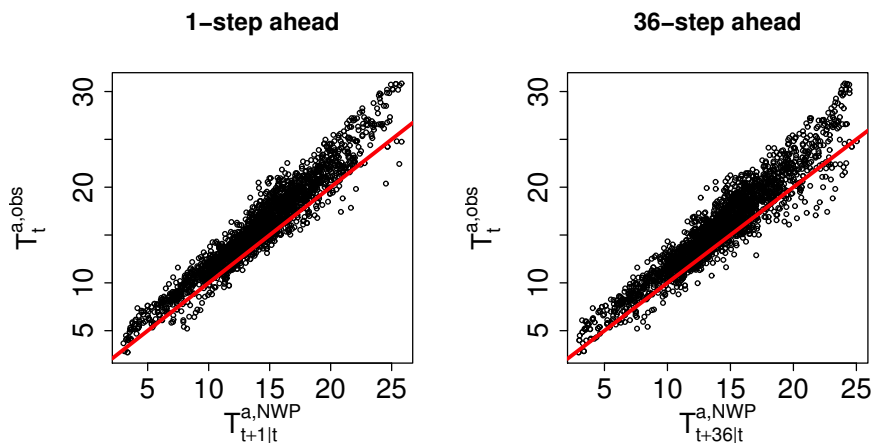


Figure 2.5: Scatterplots of the observed temperature versus the NWP for 1-step ahead (left plot) and 36-step ahead (right plot), including a line with the slope of 1 and intercept 0.

The way to handle this, is to fit the NWP to the observed ambient temperature, by using the function `loess()` in the statistic software called R¹.

The function `loess()` fit a non-parametric local polynomial regression model, using locally weighted least squares, that gives more weight to points near the point being fitted. The amount of nearby points is determined by the parameter *span*, which determines the degree of smoothness.

With the span equal to 0.9, the result displayed in Figure 2.6 is obtained, this is done for all k , from 1 to 42, the NWP are further on denoted in the same way, $T_{t+k|t}^{a,nwp}$.

When a forecast is calculated at time t , past values of the inputs are being used, in order to do this, the observed ambient temperature are combined with the NWP. The combining is achieved by forming a time series at time t , for a

¹R is a free software for statistical computing and graphics, and is available here <http://www.r-project.org>

specific horizon k , denoted

$$\{T_{t+k|t}^a\} = \{\dots, T_{t-1}^{a,obs}, T_t^{a,obs}, T_{t+1|t}^{a,nwp}, T_{t+2|t}^{a,nwp}, \dots, T_{t+k|t}^{a,nwp}\} \quad (2.2)$$

Now it is possible to include dynamics in the system in an efficient way, i.e. by being low-pass filtered as explained in Section 4.1.1.

The quality of the predicted ambient temperature is investigated, by deriving the Root Mean Square Error (RMSE), which is defined as

$$RMSE_k = \sqrt{\frac{1}{N} \sum_{t=1}^N \epsilon_{t+k}^2} \quad (2.3)$$

The $RMSE_k$ that is being investigated, is the Root Mean Square of the difference between the observed ambient temperature and the predicted k -th horizon 1 to 42. Where the observed ambient temperature has been fitted, as a function of the NWP, by `loess()`.

In Figure 2.6 the ambient temperature is plotted against the NWP for k -step 1 and k -step 36, together with the `loess` fit for three different spans, 0.5, 0.7 and 0.9.

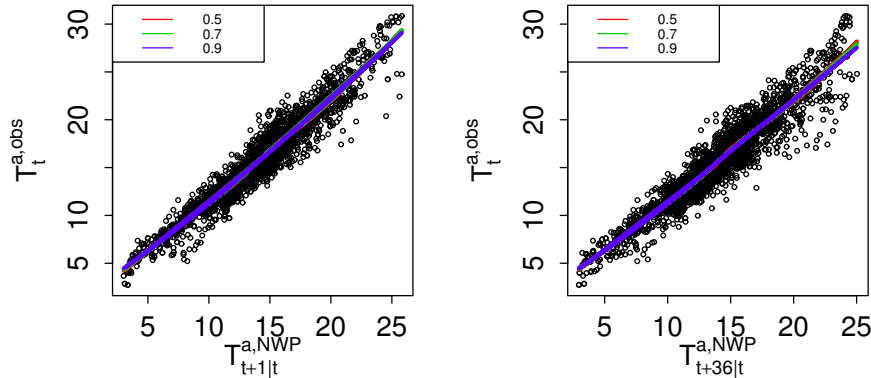


Figure 2.6: Scatterplot of ambient temperature as a function of predicted ambient temperature 1-step ahead to the left and 36-step ahead to the right, inclusive the loess fitted values, with different spans.

From this it is seen that, in this case, the span does not have a significant impact on the fit, even if there is a little spread between them in the end, for the 36-step predicted temperature, this is not found to be significant. So the span is picked to be 0.9.

Then the $RMSE_k$ for horizon 1 to 42 are calculated, with the `loess` fitted observations from the selected period and displayed in Figure 2.7.

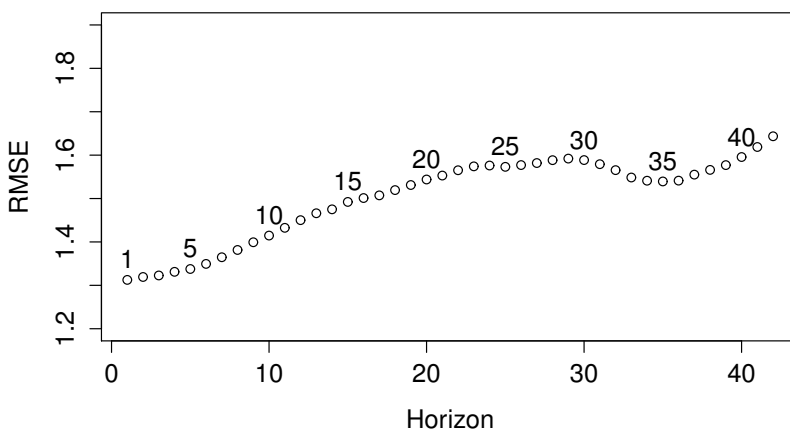


Figure 2.7: $RMSE_k$ for the difference between the loess fitted ambient temperature and predicted temperature from period May 1st to August 1st 2012, for horizon 1 to 42.

It is clearly seen that the predictions, made by DMI, for approximately horizon 20 to 30 have an unexpected decrease in performance, especially considering the better performance in the longer horizons, such as k-step 34, 35 and 36. This is presumably a random effect occurring in the three months period, with a couple of bad predictions, and due to the scheduled time for running the model. The predictions are updated only four times a day, so the same predictions are used for some of the same steps, then there will be some correlation between the RMSE for those steps. To investigate this the same $RMSE_k$ calculations are conducted for all the acquired data and displayed in Figure 2.8

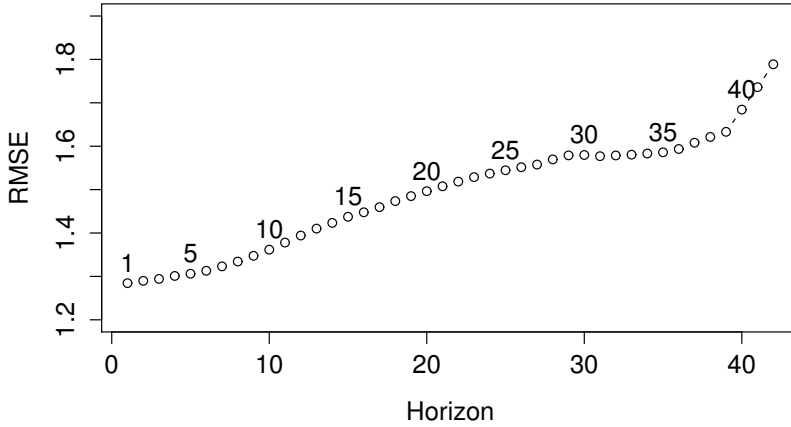


Figure 2.8: $RMSE_k$ for the difference between the loess fitted ambient temperature and predicted temperature from the whole period, for horizon 1 to 42.

From this it is clearly seen that the odd pattern from before is gone, hence it is found to be a random effect for the selected period. The selected period from May 1st to August 1st 2012, will still be used for modelling in this thesis, but it is kept in mind, that this pattern might show up when evaluating the models later on.

2.4 Replacements of missing data

As seen in Figure 2.2, there are still data missing, but since the gaps are rather small and the quantities are small, they are simply replaced.

There are two slightly larger periods, which is a two day period from May 12th to May 14th and an one day period from June 28th to June 29th, where the load measurements are missing. These periods are filled with data corresponding to the same hours and weekdays, from the week before. All the corresponding weather data is also replaced, so the weather corresponding to the load, are copied. Then there is approximately 10 small gaps of 1-2 hours length, these are replaced with the corresponding hour from the day before, and the same goes for the weather data.

These replacements, will of course give rise to a slight increase in the forecasting error, because they are not the correct measurements, but the amount is so small compared to the total amount of data, so the error will be insignificant. In Figure 2.9, data is displayed, with before replacements on top and after replacements at the bottom.

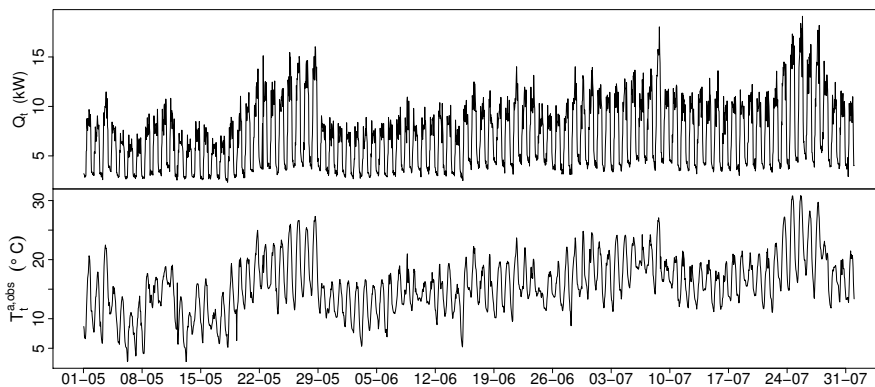


Figure 2.9: Time series plots of the load, before gaps are replaced (top) and after gaps are replaced (bottom).

2.5 Exploratory analysis

A way to obtain useful information, is to investigate the dependency between the measured refrigeration load and the ambient temperature. This is carried out by plotting them against each other with `loess` fitted red lines, seen in Figure 2.10, where the load and ambient temperature is divided in opening and closing hours.

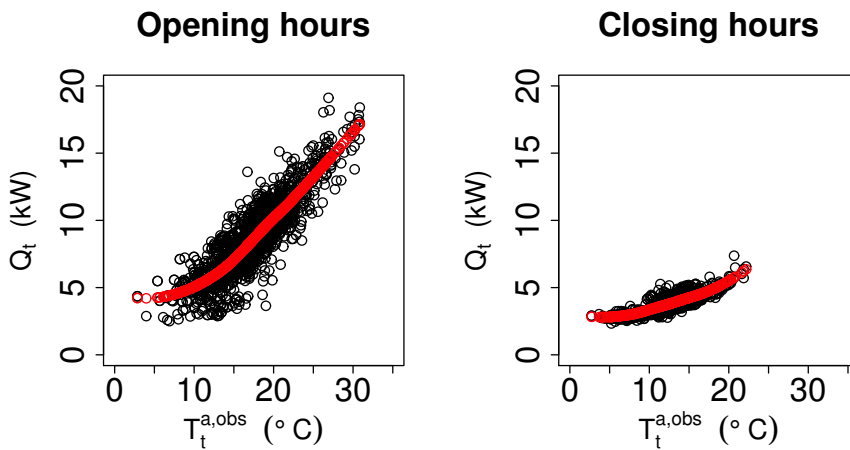


Figure 2.10: Ambient temperature versus load, for opening hours (left) and closing hours (right), with a loess fit curve.

From these plots a non-linear dependency is clearly seen, especially in closing hours. This needs to be taking into account when modelling a forecast model.

CHAPTER 3

Autoregressive Integrated Moving Average model

In this chapter a suitable linear stochastic model (i.e. no external inputs) is identified and based on the observed refrigeration load, described in Section 2.1, an Autoregressive Integrated Moving Average model (ARIMA), which is called an adjusted version of random walk and random trend models, is found suitable. Often it is not possible to describe observations as generated by a stationary process, due to seasonal trends and general time-varying behaviour, so therefore the most general class of models for forecasting a non-stationary time series, the ARIMA model, is applied.

These models needs a stationary time series, which can be obtained by transformations such as differencing and logarithmic transformation and when there is a seasonal behaviour, a multiplicative seasonal ARIMA model would be suitable. From (Madsen, 2008, p. 132), the following definition, for a multiplicative seasonal model is obtained.

3.1 DEFINITION (ARIMA $(p, d, q) \times (P, D, Q)_s$)

The process $\{Y_t\}$ is said to follow a multiplicative $(p, d, q) \times (P, D, Q)_s$ seasonal model if

$$\phi(B)\Phi(B^s)\nabla^d\nabla_s^D Y_t = \theta(B)\Theta(B^s)\epsilon_t, \quad (d, D, s \in N) \quad (3.1)$$

where $\{\epsilon_t\}$ is white noise, ϕ and θ are a polynomials of order p and q , respectively, and Φ and Θ are polynomials of order P and Q , which have all the roots inside the unit circle.

B is the backward shift operator, where $B^k Y_t = Y_{t-k}$.

Lags of the differenced series appearing in the model are called "autoregressive" terms, p and P , lags of the errors are called "moving average" terms, q and Q , and the times series differenced to be made stationary is called an "integrated" version of a stationary series, d and D . The season is denoted by s .

First the methods used for the modelling are presented in Section 3.1, then in Section 3.2, the model building step by step, are outlined and at last in Section 3.3 the selected model is used for forecasting, where the performance is evaluated.

3.1 Methods

The procedure used for model building, is a three stage procedure displayed in Figure 3.1.

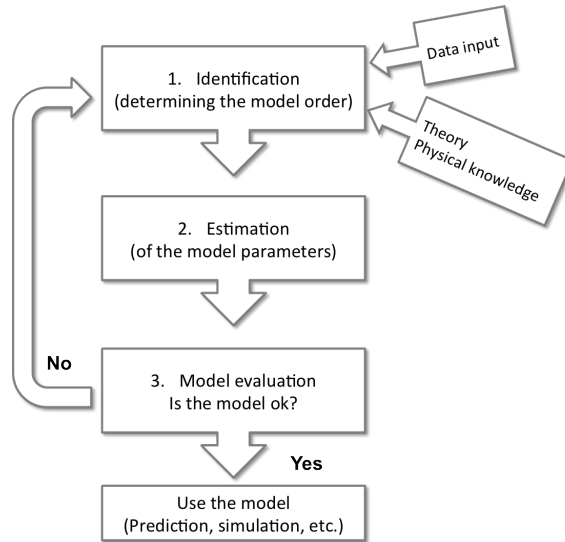


Figure 3.1: The model building procedure.

The first stage, is identification, this involves determining the model order, which is based on information from data together with knowledge about the physics driving the process. An initial identification is mainly based on the estimated autocorrelation function, explained in Section 3.1.1, where it is used to detect if a transformation is needed, see Section 3.1.2, and to investigate if differencing is needed, hereafter the orders are identified.

Second stage is parameter estimation, after the model order is determined the parameters are estimated with use of Maximum likelihood methods (ML method), see 3.1.3.

Last stage is to test the model, to see if it is an adequate model or if something more can be changed to make it better. There are several number of tools for testing the model, in this thesis a residual analysis will be conducted, testing whether the residuals can be assumed to be white noise. This is carried out by plotting the residuals to check for non-stationarities and outliers, plotting the autocorrelation function with the 95% confidence interval and test if the individual autocorrelations are significantly different from zero. The cumulative

periodogram is calculated and plotted, to check if the residuals can be assumed to be white noise.

If all tests are acceptable and no further improvement can be achieved, then the model is used for forecasting.

In this current Section, the relevant tools used for model building and testing, is presented.

3.1.1 Autocorrelation function and partial autocorrelation function

The autocorrelation function, ACF, is defined, from (Madsen, 2008, p. 103), as

$$\rho_{XX}(t_1, t_2) = \frac{\text{cov}[X(t_1), X(t_2)]}{\sqrt{\sigma^2(t_1)\sigma^2(t_2)}} \quad (3.2)$$

This gives the correlation between lagged values in a time series, which can be used for detecting seasonal trends, non-stationarity and the order of the model. Another useful measure, is the Partial Autocorrelation function, PACF, which is defined as, (Madsen, 2008, p.124)

$$\phi_{kk} = \text{Cor}[Y_t, Y_{t+k} | Y_{t+1}, \dots, Y_{t+k-1}] \quad (3.3)$$

This is the partial correlation coefficients between the series, which describes the amount of correlation between a variable and a lag of itself which is not explained by correlations in all lower order lags. For example, it is expected that the correlation at lag 1, will propagate to lag 2 and probably to higher order lags, then the partial autocorrelation at lag 2 is the difference between the actual correlation at lag 2 and expected correlation due to propagation of correlation at lag 1.

This is specially useful to identify the order of the autoregressive term needed in the model.

3.1.2 Box-Cox transformation

The Box-Cox transformation is used to stabilize the variance, so the normality of data is improved.

This transformation has the form:

$$Y_t^{(\lambda)} = \begin{cases} (Y_t^\lambda - 1)/\lambda & \lambda \neq 0 \\ \ln Y_t & \lambda = 0 \end{cases} \quad (3.4)$$

The method used for examining if this kind of transformation is needed, is a range-mean plot.

Range-mean plot method

First the data is divided sequentially into groups consisting of n observations, e.g. monthly data is divided into month groups; May, June etc. or hourly data is divided into hour groups; 01:00, 02:00 etc.

Then the range $Y_{max} - Y_{min}$ and the mean value are calculated in each group. These are plotted in a range-mean plot.

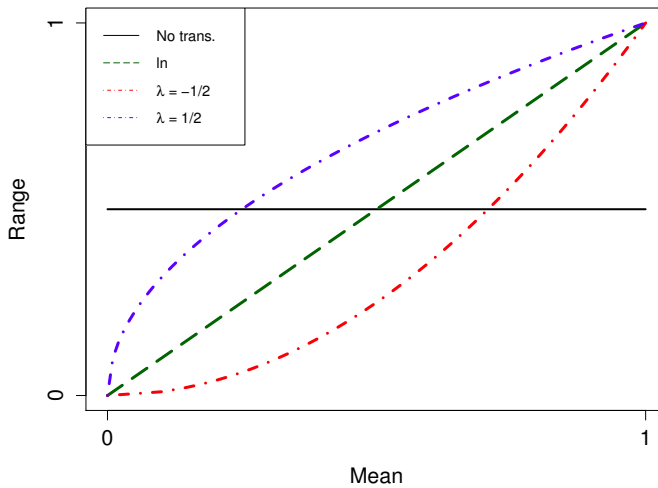


Figure 3.2: Box-Cox transformation patterns.

In Figure 3.2, the Box-Cox transformations for different range-mean relations are illustrated. If the range and mean values are independent then no transformation is needed ($\lambda = 1$), but if any dependency is detected a transformation should be considered. A (positive) linear dependency indicates that a logarithmic transformation ($\lambda = 0$) should be applied, and upwards or downwards curvature indicates that, $\lambda = -1/2$ and $\lambda = 1/2$ should be applied, respectively, (Madsen, 2008)

If the curvature, up or down, are more extreme than displayed in Figure 3.2,

then λ should be decreased or increased, respectively.

3.1.3 Parameter estimation method

The method used, for estimating the parameters in an ARIMA model is the Maximum Likelihood method (ML method). The method requires an assumption of the distribution, which in general is that $\{\epsilon_t\}$ is I.I.D normally distributed (i.e. white noise) with variance $Var[\epsilon_t] = \sigma_\epsilon^2$.

All observations and a given set of parameters are denoted \mathbf{Y}_N and $\boldsymbol{\theta}$ respectively.

The loglikelihood function is then (Madsen, 2008)

$$\log L(\mathbf{Y}_N; \boldsymbol{\theta}; \sigma_\epsilon^2) = -\frac{N-p}{2} \log(\sigma_\epsilon^2) - \frac{1}{2\sigma_\epsilon^2} \sum_{t=p+1}^N \epsilon_t^2(\boldsymbol{\theta}) + c \quad (3.5)$$

where c is constant, the minimum is obtained for

$$\hat{\sigma}_\epsilon^2 = \left(\sum_{t=p+1}^N \epsilon_t^2(\boldsymbol{\theta}) \right) / (N-p) \quad (3.6)$$

inserting into (3.5) gives

$$\log L(\mathbf{Y}_N; \boldsymbol{\theta}; \hat{\sigma}_\epsilon^2) = -\frac{(N-p)}{2} \log \left(\sum_{t=p+1}^N \epsilon_t^2(\boldsymbol{\theta}) \right) + c \quad (3.7)$$

This yields that the ML estimates is obtained by minimizing

$$S(\boldsymbol{\theta}) = \sum_{t=p+1}^N \epsilon_t^2(\boldsymbol{\theta}), \quad (3.8)$$

where the ML estimate for σ_ϵ^2 is obtained by

$$\hat{\sigma}_\epsilon^2 = \frac{S(\hat{\boldsymbol{\theta}})}{N-p} \quad (3.9)$$

One of the properties for the MLE (Maximum Likelihood Estimator) is consistency, which means that with a sufficiently large number of observations N , it is possible to find estimates that is close to the true value, i.e. when N goes to infinity the estimator converges in probability to its true value.

This method is conducted in the statistical program R¹, with the use of the function `arima()`.

¹<http://www.r-project.org>

3.1.4 Test for lower order model

When estimating a model parameter, the variance of the estimate is also determined. Since the estimated parameters can be assumed to be asymptotically normally distributed, it is possible to test whether a parameter θ_i is significantly different from zero. This is conducted by testing the hypothesis

$$H_0 : \theta_i = 0 \quad \text{against} \quad H_1 : \theta_i \neq 0 \quad (3.10)$$

with the test statistic

$$F = T^2 = \frac{\hat{\theta}_i}{\hat{\sigma}_{\hat{\theta}_i}} \quad (3.11)$$

which under H_0 follows a $F(1, f)$ -distribution with $f = N - p - q$ degrees of freedom, where N is the number of observations used in the estimation of θ_i , for further details (see Madsen, 2008).

3.2 Model identification, estimation and evaluation

When identifying a model for a linear stochastic process, it is vital that the observations are stationary. It is observed in Figure 2.2, that the variance in the observations are not constant and there is a small increase in the mean value, which indicates non-stationarity. From this, it will be ideal to first examine if a Box-Cox transformation is needed, which will establish a constant variance, see Section 3.1.2.

First a range-mean plot is created, with groups of each hour, i.e. all observations from hour 01:00 are in a group and hour 02:00 are in a group, etc. Then the mean value and the range are calculated for each group, and gives the plot in Figure 3.3

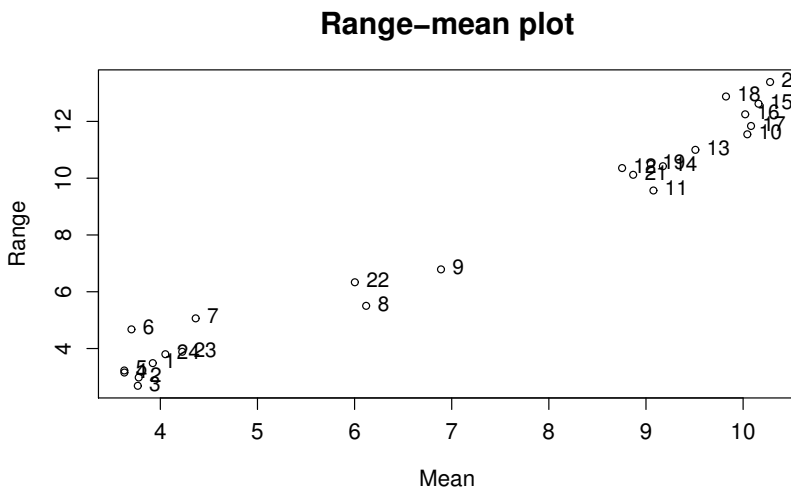


Figure 3.3: Range-mean plot, with 24 groups.

From this plot, a linear relationship between the range and the mean value of the power load, is observed, which indicates that a logarithmic transformation should be considered, see Figure 3.2.

So the observations are transformed

$$\{Q_t^T = \ln(Q_t), \quad t = 1, \dots, N\}$$

where $N = 2208$.

The variance are more constant now, still a little increase in the mean value, see Figure 3.4, due to this increase, the autocorrelation function, ACF, is estimated.

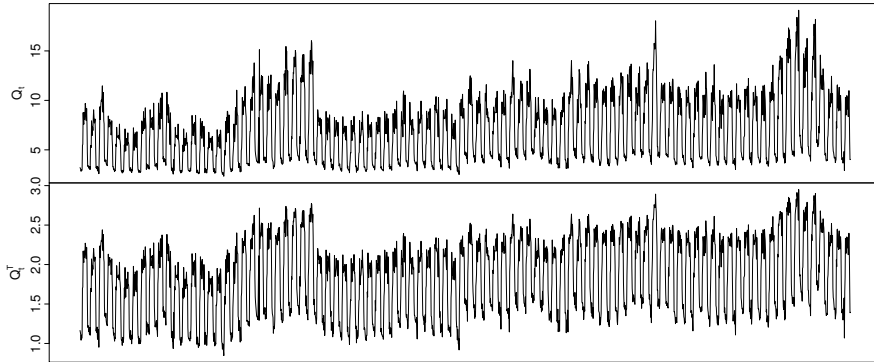


Figure 3.4: The upper figure is with the originally observed hourly load consumption and the lower figure are the logarithm of the hourly load consumption.

The estimated ACF for a sub-part and the entire series, are shown in Figure 3.5

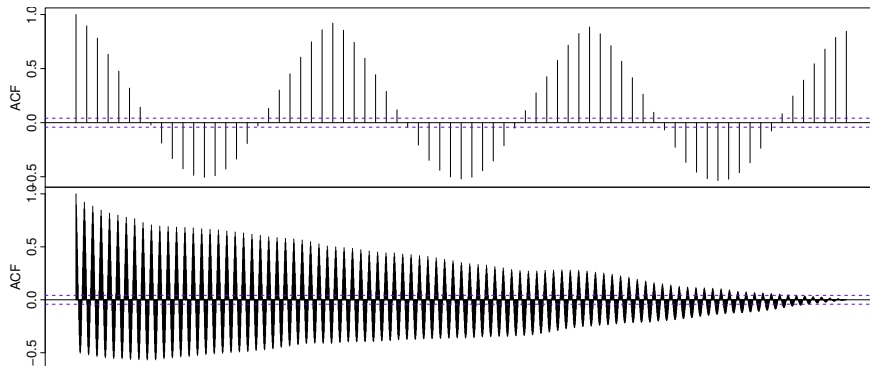


Figure 3.5: The upper figure shows the ACF for 72 lags and the lower figure shows for the entire series.

The ACF is characterized by a period of 24 hours, and the values moves slowly towards 0, which indicates that the series is still non-stationary and that a differencing is needed. So the first differencing of the observations are as follows

$$\nabla Q_t^T = Q_t^T - Q_{t-1}^T$$

This differencing is shown as the plot at the top left corner of Figure 3.6, to-

gether with the corresponding ACF (top right corner). It is seen that the non-stationarity has been removed with the differencing, but a seasonal differencing, by lag 24, is needed to remove the spikes at lag 24, 48, 72, ... etc. Which is calculated as

$$\nabla\nabla^{24}Q_t^T = (Q_t^T - Q_{t-1}^T) - Q_{t-24}^T$$

The seasonal differencing is displayed in Figure 3.6 as the two plots in the bottom.

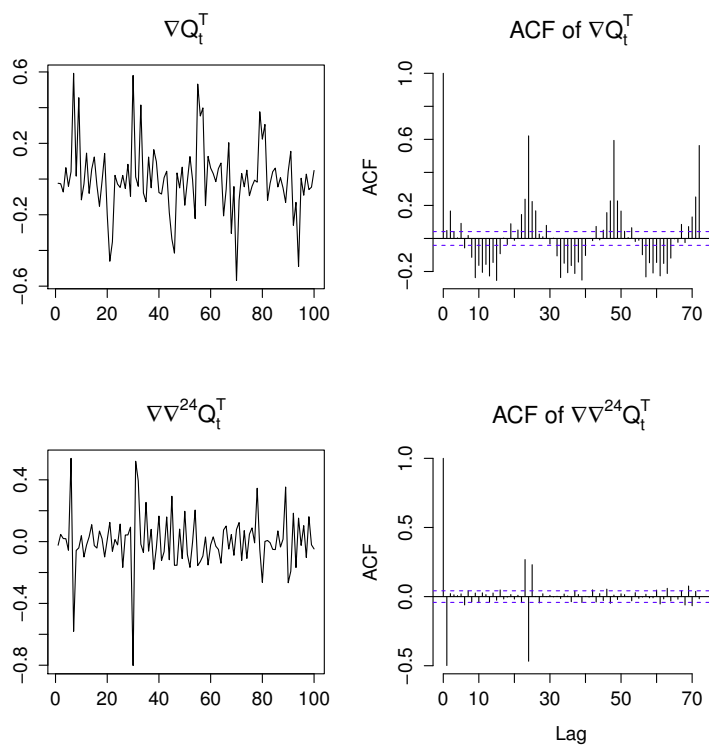


Figure 3.6: Plots of a sub-part of the differenced series and corresponding ACF plot.

Now the series $\nabla\nabla^{24}Q_t^T$ is found to be stationary, the next step is to determine the orders of the polynomials in the autoregressive model. There are two large values of the ACF, for $\nabla\nabla^{24}Q_t^T$, in lag 1 and lag 24, which implies that the series is slightly over-differenced, this will be partly cancelled out by a $MA(1)$ and $MA(1)_{24}$ term. So initially the following model, denoted by

$ARIMA_{(0,1,1) \times (0,1,1)_{24}}$, is applied.

$$\nabla \nabla_{24} Q_t^T = (1 + \theta_1 B)(1 + \Theta_1 B^{24}) \epsilon_t \quad (3.12)$$

Where B is the backward shift operator defined in the beginning of Chapter 3, the parameters are estimated with the ML method and displayed in Table 3.1, see 3.1 for more detailed description of method. This model has a standard deviation of $\hat{\sigma}^2 = 0.0133$.

Table 3.1: Parameter estimates and standard errors for model $ARIMA_{(0,1,1) \times (0,1,1)_{24}}$.

Parameter	Value	$\hat{\sigma}$
$\hat{\theta}_1$	-0.6492	0.0176
$\hat{\Theta}_1$	-0.9512	0.0135

When doing a lower order test, explained in Section 3.1.4, the test statistic should be $F(1, 2006)$ -distributed, ie. $T^2 < F_{0.05}(1, 2006) \approx 3.84$. The test values for θ_1 and Θ_1 are 36.886 and 70.459 respectively, so the null hypothesis is rejected and the parameters are accepted in to the model.

The residuals are now analysed, to see if they satisfy the criteria of being white noise and if there is any unexplained correlation. In Figure 3.7 these residuals are plotted, together with the corresponding ACF, PACF and a cumulative periodogram.

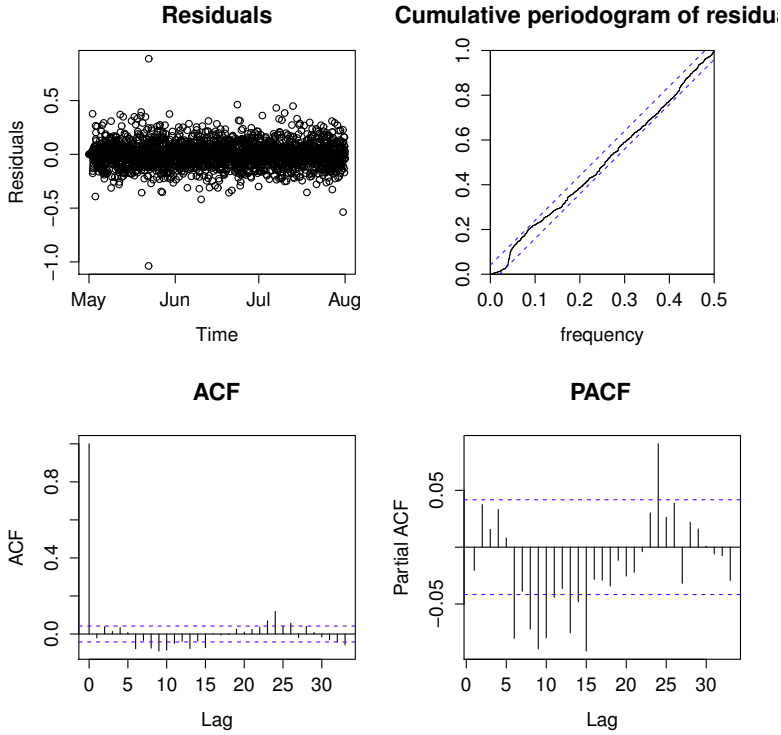


Figure 3.7: Residuals, cumulative periodogram, ACF and PACF plot for $ARIMA_{(0,1,1) \times (0,1,1)_{24}}$.

From this it is seen that, there is still some correlation not being described by the model in lag 24, even though the residuals looks like white noise with only two potential outliers, and the cumulative periodogram of the residuals is within the bands. Which leads to model, $ARIMA_{(0,1,1) \times (1,1,1)_{24}}$, where a seasonal AR term is added to the model:

$$(1 - \Phi_1 B^{24}) \nabla \nabla_{24} Q_t^T = (1 + \theta_1 B)(1 + \Theta_1 B^{24}) \epsilon_t \quad (3.13)$$

The standard deviation are now $\hat{\sigma}^2 = 0.0130$ with the parameter estimates, listed in Table 3.2.

Table 3.2: Parameter estimates and standard errors, for model $ARIMA_{(0,1,1) \times (1,1,1)_{24}}$.

Parameter	Value	$\hat{\sigma}$
$\hat{\Phi}_1$	0.1476	0.0229
$\hat{\theta}_1$	-0.6619	0.0176
$\hat{\Theta}_1$	-0.9796	0.0120

Checking this model for lower order, gives the test statistics 6.445, 37.608 and 81.633 for the parameters respectively, which is larger than $F_{0.05}(1, 2005) \approx 3.84$ and are therefore accepted into the model.

There is a very small improvement in the standard deviation compared to $ARIMA_{(0,1,1) \times (0,1,1)_{24}}$, and when looking at the residuals analysis in Figure 3.8 it is seen that the significant large spike in lag 24 are now small enough to conclude being described by the model. The residuals are white noise like, and the cumulative periodogram shows that the model is adequate.

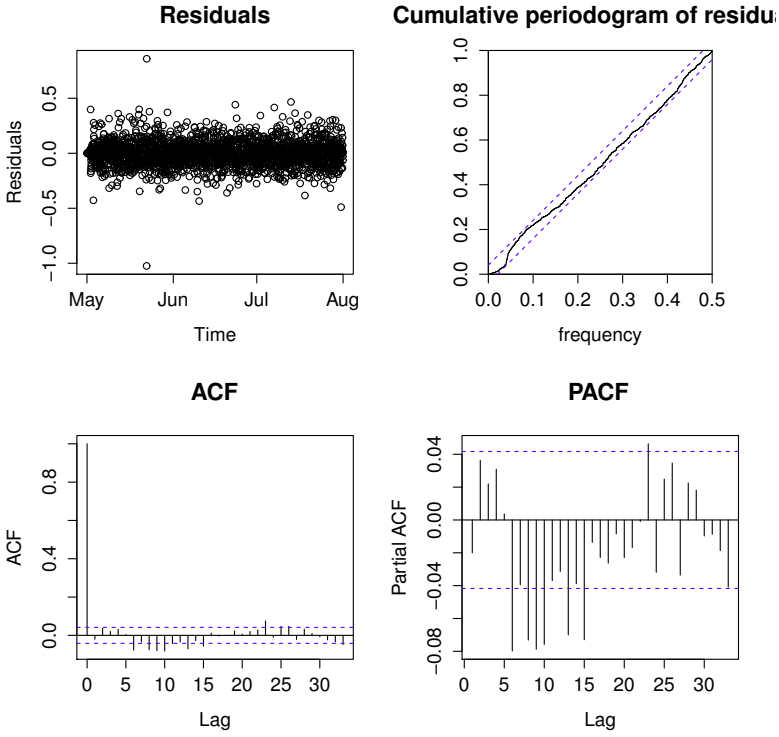


Figure 3.8: Residuals, cumulative periodogram, ACF and PACF for $ARIMA_{(0,1,1) \times (1,1,1)_{24}}$.

There is still some significant spikes in the ACF and PACF, there is a sharp cutoff from lag 6 to 15 in the PACF, so a AR(6) term would be appropriate to test, next model to be tested is $ARIMA_{(6,1,1) \times (1,1,1)_{24}}$

$$\phi(B)(1 - \Phi_1 B^{24}) \nabla \nabla_{24} Q_t^T = (1 + \theta_1 B)(1 + \Theta_1 B^{24}) \epsilon_t \quad (3.14)$$

where $\phi(B) = 1 - \phi_1 B - \phi_2 B^2 - \phi_3 B^3 - \phi_4 B^4 - \phi_5 B^5 - \phi_6 B^6$.

The standard deviation has decreased with approximately 4%, to $\hat{\sigma}^2 = 0.0125$. The parameter values are estimated and displayed in Table 3.3 below.

Table 3.3: Parameter estimates and standard errors, for model $ARIMA_{(6,1,1) \times (1,1,1)_{24}}$.

Parameter	Value	$\hat{\sigma}$
$\hat{\Phi}_1$	0.1427	0.0229
$\hat{\theta}_1$	-0.9416	0.0134
$\hat{\Theta}_1$	-0.9861	0.0150
$\hat{\phi}_1$	0.2355	0.0249
$\hat{\phi}_2$	0.2113	0.0237
$\hat{\phi}_3$	0.1270	0.0232
$\hat{\phi}_4$	0.0924	0.0229
$\hat{\phi}_5$	0.0266	0.0225
$\hat{\phi}_6$	-0.0733	0.0222

The previous parameters are still significant, a lot of the new parameter values also looks acceptable, except for $\hat{\phi}_5$, here the parameter value are only a little higher than the standard error and $\hat{\phi}_6$ is also close to being unacceptable. So there is a large possibility that these parameters does not increase the performance of the model, and therefore a great potential for excluding these. When looking at the residual analysis in Figure 3.9, it looks acceptable.

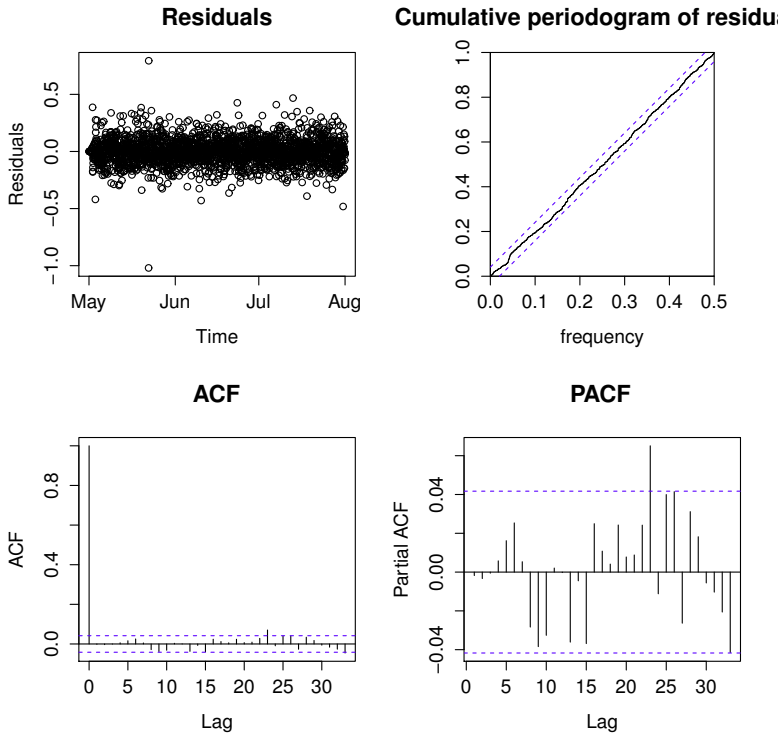


Figure 3.9: Residuals, cumulative periodogram, ACF and PACF for $ARIMA_{(6,1,1) \times (1,1,1)_{24}}$.

There is still some correlation in lag 23, but it is very small and it will be very difficult to do something about that correlation. The cumulative periodogram looks better, where the small "waves" in the beginning are reduced, so now it looks more like white noise, than the previous model. It would be a good thing to test for lower order model now, because the simplest model possible, without too much disruption in the residuals, is preferred to ensure computational efficiency. The test is explained in Section 3.1.4 and in this case the null hypothesis is rejected if the test statistic is larger than $F_{0.05}(1, 2201) \approx 3.84$. The results are presented in Table 3.4

Table 3.4: Results from the test for lower order model, with parameters from $ARIMA_{(6,1,1) \times (1,1,1)}$.

Parameter	Test statistic	$H_0 : \theta_i = 0$
$\hat{\Phi}_1$	$F = \frac{0.1427}{0.0229} = 6.231$	reject
$\hat{\theta}_1$	$F = \frac{0.9416}{0.0134} = 70.269$	reject
$\hat{\Theta}_1$	$F = \frac{0.9861}{0.0150} = 65.740$	reject
$\hat{\phi}_1$	$F = \frac{0.2355}{0.0249} = 9.458$	reject
$\hat{\phi}_2$	$F = \frac{0.2113}{0.0237} = 8.916$	reject
$\hat{\phi}_3$	$F = \frac{0.1270}{0.0232} = 5.474$	reject
$\hat{\phi}_4$	$F = \frac{0.0924}{0.0229} = 4.035$	reject
$\hat{\phi}_5$	$F = \frac{0.0266}{0.0225} = 1.182$	accept
$\hat{\phi}_6$	$F = \frac{0.0733}{0.0222} = 3.302$	accept

From this test, it is concluded that $\hat{\phi}_5$ and $\hat{\phi}_6$ should be excluded from the model, because they do not increase the performance significantly, $\hat{\phi}_4$ is also very close to being accepted as zero, so this will also be excluded, for more simplicity. The model now identified is $ARIMA_{(3,1,1) \times (1,1,1)_{24}}$

$$\phi(B)(1 - \Phi_1 B^{24}) \nabla \nabla_{24} Q_t^T = (1 + \theta_1 B)(1 + \Theta_1 B^{24}) \epsilon_t \quad (3.15)$$

where $\phi(B) = 1 - \phi_1 B - \phi_2 B^2 - \phi_3 B^3$.

This model has a standard deviation of 0.01267, which is a small increase from the last model. The parameter estimates together with the lower order test, are displayed in table 3.5.

Table 3.5: Parameter estimates, standard deviation and test statistics for model $ARIMA_{(3,1,1) \times (1,1,1)_{24}}$.

Parameter	Value	$\hat{\sigma}$	Test statistic
$\hat{\Phi}_1$	0.1451	0.0228	6.364
$\hat{\theta}_1$	-0.9374	0.0127	73.811
$\hat{\Theta}_1$	-0.9873	0.0161	61.323
$\hat{\phi}_1$	0.2419	0.0252	9.599
$\hat{\phi}_2$	0.2207	0.0241	9.158
$\hat{\phi}_3$	0.1366	0.0233	5.862

Now all parameters are rejected to be zero, so they will be kept in the model, even though the standard deviation of the model increased slightly, it is better to have a simpler model, with less parameters. From the residual analysis, displayed in Figure 3.10, it is seen that they still look like white noise, there are now some small correlation in lag 4 and 5, but it is known that they will not have any positive effect on the model.

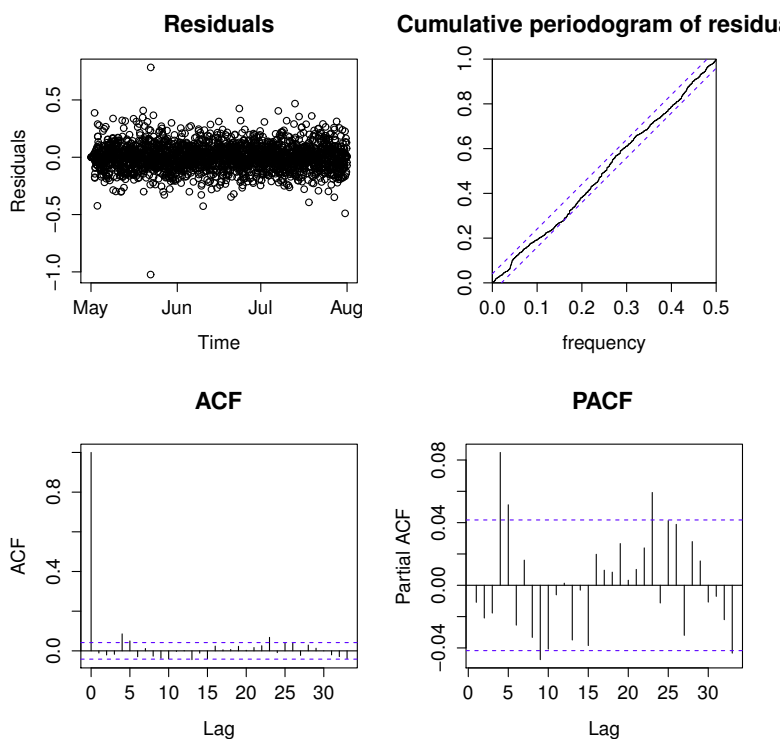


Figure 3.10: Residuals, cumulative periodogram, ACF and PACF for $ARIMA_{(3,1,1) \times (1,1,1)_{24}}$.

There is no clear way, from the analysis, to improve this model, hence the model selection is ended and the model $ARIMA_{(3,1,1) \times (1,1,1)_{24}}$ is selected as the most suitable autoregressive model for this data, and then used for prediction in Section 3.3.

3.3 Model performance

Now that a model has been identified and the parameters have been estimated, the model is applied for forecasting. The forecast is carried out up to 48 steps ahead, for the period from August 1st to 3th. The result, after being transformed back to load, is listed in Table 3.6 and displayed in Figure 3.11

Table 3.6: Predicted load in kW, for horizon 1 to 48.

Step k	Load $\hat{Q}_{t+k t}$	Step k	Load $\hat{Q}_{t+k t}$	Step k	Load $\hat{Q}_{t+k t}$	Step k	Load $\hat{Q}_{t+k t}$
1	3.91	13	9.39	25	3.92	37	9.42
2	3.80	14	9.29	26	3.79	38	9.14
3	3.72	15	9.90	27	3.76	39	10.03
4	3.66	16	9.97	28	3.64	40	9.94
5	3.63	17	9.95	29	3.63	41	9.96
6	3.84	18	9.47	30	3.73	42	9.65
7	4.01	19	9.08	31	4.22	43	8.97
8	5.97	20	10.30	32	6.10	44	10.21
9	6.78	21	8.88	33	6.87	45	8.84
10	10.07	22	5.96	34	10.05	46	5.97
11	8.99	23	4.18	35	9.03	47	4.21
12	8.65	24	4.05	36	8.68	48	4.06

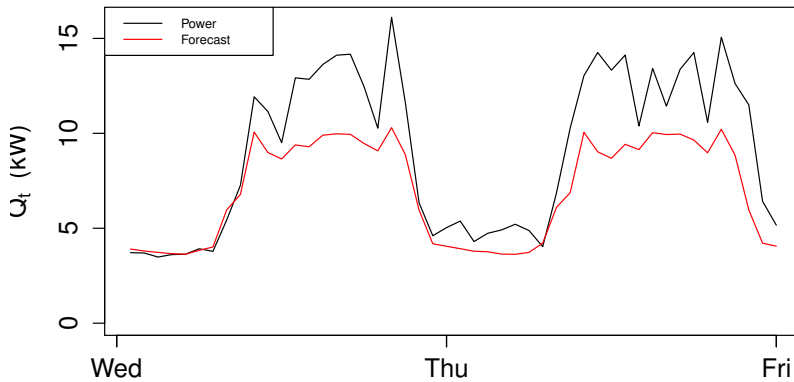


Figure 3.11: The predicted refrigeration load and the observed refrigeration load.

From this it is seen that the prediction error, increases with the predicted horizon, since the observation inputs are replaced with predictions, when longer horizons are predicted. This gives a high uncertainty and therefore larger residuals, the further away from the newest observations, the horizon gets.

No NWP's are used as external input, because when adding an external input to an ARIMA model, it is added as a linear regression and from Section 2.5, it was discovered that there is no linear dependency between the load and the NWP's, therefore no improvement in the performance will be seen, from adding NWP's as external input.

If this model should be an adequate model, for forecasting of refrigeration load, then the newest observations should be available and uploaded into the model very often, almost every hour or every second hour, this is time demanding and computational heavy. Therefore a more non-linear approach, with grey model (a linear model with non-linear inputs), will be tested, to see if these are able to make a more stable forecast on larger horizons.

Adaptive Linear Model

In this chapter an adaptive linear time-series model is presented and used as basis for three other adaptive linear time-series models. Each model is fitted with a computationally efficient recursive least squares scheme. With a starting point in the model studied by Bacher et al. (2013), presented in Section 4.2, the other three models takes there origins and are presented in Section 4.3, 4.4 and 4.5. All models have regime switching and a diurnal curve in common, and then the dynamic relations between the ambient temperature and the refrigeration load is modelled in different ways, in order to find the best suitable model for the refrigeration load forecasting.

The chapter is structured in the following way; first the methods used for the modelling is presented, then each model is presented in separate sections, in which each model is described and evaluated. This evaluation will then be followed up by Chapter 5 and 6.

4.1 Methods

In this Section the methods used for the adaptive linear time-series models are presented.

4.1.1 First order low-pass filtering

The heat dynamics of a building can be described by lumped parameter RC-models, see for example Madsen and Holst (1995), Braun and Chaturvedi (2002) and Jiménez et al. (2008). Due to the fact that the refrigerators and coolers are placed inside a building, the response in the load to changes in the climate variables can be modelled with rational transfer functions. The following is a description of the low-pass filtering effect of the building with an RC-model. The simplest first order low-pass filter, with a stationary gain of one, is a model of the building heat dynamics formed by an RC-model with a single resistor and a single capacitor. A low-pass filter is a filter where the slow variations pass undisturbed, while the fast variations are damped. As an example the transfer function from the ambient temperature to the refrigeration load is

$$Q_t = \alpha_a H_a(q) T_t^a \quad (4.1)$$

with

$$H_a(q) = \frac{1 - a_{T_a}}{1 - a_{T_a} q^{-1}} \quad (4.2)$$

and where q^{-1} is the backward shift operator, defined by Equation (3.1), page 18, α_a is the stationary gain from the ambient temperature to load and $a_{T_a} \in [0, 1]$ is a parameter which is corresponding to the time constant for the part of the system affected by change in ambient temperature. If the system has a high thermal mass and good insulation, a relatively high a_{T_a} is expected, thus the filter parameter needs to be adapted for each system in order to describe the dynamics properly. These filters are adapted to match the response of the system to each effect separately.

4.1.2 Recursive Least Squares with forgetting

As time passes and more information becomes available, it is often preferred to be able to update the model parameter estimates. A way to do this is to use a recursive least squares (RLS) scheme with forgetting, as described in the article from Bacher et al. (2009), this makes it possible for the parameters to change over time and adapt to changing conditions. It is a recursive implementation of a weighted least squares estimation, where the weights are exponentially decaying over time. The algorithm used to update the parameters is defined as (Madsen, 2008, page 317)

4.1 DEFINITION (RLS ALGORITHM WITH FORGETTING)

$$\hat{\theta}_t = \hat{\theta}_{t-1} + \mathbf{R}_t^{-1} \mathbf{X}_t [Y_t - \mathbf{X}_t^T \hat{\theta}_{t-1}] \quad (4.3)$$

$$\mathbf{R}_t = w(\Delta t) \mathbf{R}_{t-1} + \mathbf{X}_t \mathbf{X}_t^T \quad (4.4)$$

where $w(\Delta t) = \lambda^{\Delta t}$, with Δt as the age of the data in hours and λ is the *forgetting factor*.

With \mathbf{X}_t as the regressor vector, θ_t as the parameter vector and Y_t is the dependent variable (observations), the k - *step* prediction at t is

$$\hat{Y}_{t+k} = \mathbf{X}_t^T \hat{\theta}_t \quad (4.5)$$

The weights $w(\Delta t) = \lambda^{\Delta t}$ implies that for $\lambda = 0.95$ they will be halved in 13 hours, for $\lambda = 0.998$ they are halved in 346 hours (~ 14 days).

With this algorithm only a few matrix operations are needed to compute the updated parameters and the associated forecast, which makes it a computationally light scheme.

4.1.3 Diurnal curve

The diurnal curve is a function applied to describe the systematic diurnal patterns in the load. This curve is modelled as a harmonic function using a Fourier series.

A Fourier series dissolves periodic functions into the sum of a set of oscillating functions, especially sines and cosines. These are very useful as a way to break up an arbitrary function into a set of simple terms that can be solved individually and then recombined to obtain the solution to the original problem. In this Thesis the following Fourier series are defined

$$\delta(t_{tod}, n_{har}, \alpha_{diu}) = \sum_{i=1}^{n_{har}} \alpha_{i,1}^{diu} \sin\left(\frac{t_{tod} i \pi}{12}\right) + \alpha_{i,2}^{diu} \cos\left(\frac{t_{tod} i \pi}{12}\right) \quad (4.6)$$

where t_{tod} is the time of day in hours at time t , n_{har} is the number of harmonics used in the Fourier series and α^{diu} is the coefficient vector for the included harmonics.

This can give the Fourier series for a square wave, which has the form similar to the one displayed in Figure 4.1.

Fourier series square wave

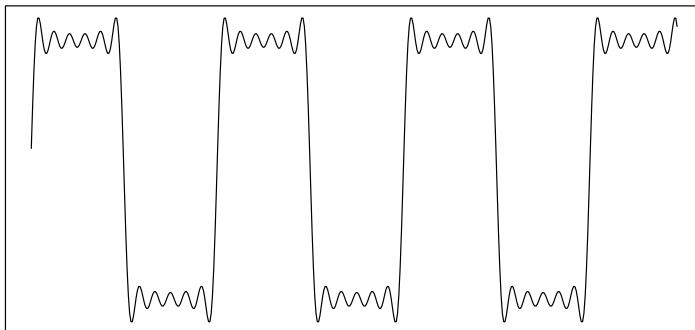


Figure 4.1: An example of a square wave Fourier series made from $\frac{4}{\pi} \sum_{n=1,3,5..}^{11} \frac{1}{n} \sin(\frac{t_{total}n\pi}{12})$.

4.1.4 Basis splines

Splines are a very effective tool for a number of approximation cases such as interpolation and data fitting. A spline is a piecewise-defined smooth polynomial function. From de Boor (2001) page 93, the following definition is obtained

4.2 DEFINITION (SPLINE FUNCTION)

A spline function of order p with knot sequence \mathbf{z} is any linear combination of B-splines of order k for the knot sequence \mathbf{z} . The collection of all such functions is denoted by $S_{p,\mathbf{z}}$ and defined as

$$S_{p,\mathbf{z}} = \left\{ \sum_j \alpha_j B_{j,p,\mathbf{z}} \quad , \alpha_j \in \mathbb{R} \text{ for } \forall j \right\}. \quad (4.7)$$

B-spline is short for Basis spline and is a piecewise-polynomial function that has minimal support with respect to a given order p and the knot sequence $\mathbf{z} = \{z_j\}_{j=1}^p$, the B-spline will further on be denoted by $B_{j,p}$. The B-spline has the property of being positive in the given interval (de Boor, 2001, p. 91).

The knots z_j , is where the polynomial pieces connect, few knots makes the

splines smoother than with many knots, however increasing the amount of knots, makes the splines more flexible to fit to data.

The B-splines of order 1 for a given knot sequence are the characteristic functions (de Boor, 2001, p.89)

$$B_{j1}(x) = X_j(x) = \begin{cases} 1, & \text{if } z_j \leq x < z_{j+1} \\ 0, & \text{otherwise} \end{cases} \quad (4.8)$$

With the constraint that the B-splines should form a **partition of unity**, i.e.

$$\sum_j B_{j1}(x) = 1. \quad (4.9)$$

In particular,

$$z_j = z_{j+1} \implies B_{j1} = 0$$

From the first-order B-splines, the higher-order B-splines are obtained by recurrence relation (de Boor, 2001, p.90)

$$B_{j,p} = \omega_{jp} B_{j,p-1} + (1 - \omega_{j+1,p}) B_{j+1,p-1} \quad (4.10)$$

with

$$\omega_{jp}(x) = \frac{x - z_j}{z_{j+k-1} - z_j} \quad (4.11)$$

for $p > 0$.

EXAMPLE 4.1 (THIRD-ORDER B-SPLINE) An example of a third-order B-spline is given by

$$\begin{aligned}
 B_{j,3} &= \omega_{j3}B_{j2} + (1 - \omega_{1+j,3})B_{j+1,2} \\
 &= \omega_{j3}\omega_{j2}X_j + (\omega_{j3}(1 - \omega_{j+1,2}) + (1 - \omega_{j+1,3})\omega_{j+1,2})X_{j+1} \\
 &\quad + (1 - \omega_{j+1,3})(1 - \omega_{j+2,2})X_{j+2} \tag{4.12}
 \end{aligned}$$

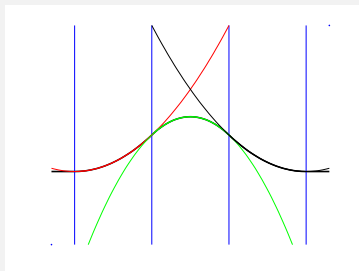


Figure 4.2: Example of a quadratic B-spline with a triple knot.

The Example 4.1 shows that B_{j3} consists of three quadratic pieces, which is joined smoothly at the knots to form a piecewise quadratic function that is zero outside the interval.

After $k-1$ steps of the recurrence, B_{jk} is obtained in the form

$$B_{jp} = \sum_{i=j}^{j+p-1} b_{ip}X_i \tag{4.13}$$

where b_{ip} are polynomials of order p .

In Figure 4.3, an example of a spline function is displayed, which is created from 1000 simulated values from the uniform distribution with a random spread, B-splines are created by the R-function `bs()`.

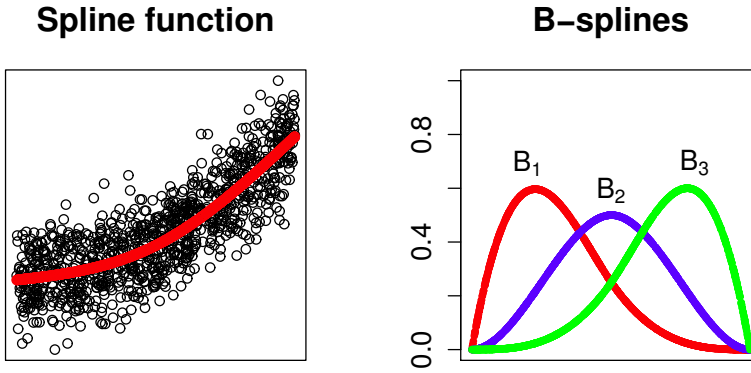


Figure 4.3: Spline function with three B-splines, from 1000 simulated values from the uniform distribution with a random spread.

In this thesis, a basis matrix B_{jp} with all the B-spline functions, will be calculated with the R-function `bs()` from the package `splines`.

4.1.5 Parameter optimization

In the following models, the parameters needs to be fitted for each prediction horizon k . The fitting is carried out in an off-line setting by minimizing $RMSE_k$, stated in Equation (2.3), page 11, for each horizon $k = 1, \dots, 42$.

This is conducted with the use of the R-function `optim()`, which is an optimization based on the quasi-Newton algorithm, this algorithm searches for the parameter values that give the smallest $RMSE_k$ by finding the stationary point of a function, where the gradient is 0.

To make the optimization calculations faster, a simple arrangement has been applied, where performing a low-pass filtering of the inputs is only carried out once for the parameter values in a given range, these series can then be used for optimization for all horizons.

In this thesis the following parameters are optimized:

- The forgetting factor from Section 4.1.2: λ

- The coefficient for the low-pass filtering from Section 4.1.1: a_{T_a}

The properties of the optimization is not studied in further details in this Thesis.

4.2 Basic Model

A previous work has been reported by Bacher et al. (2013), as mentioned in Section 1.1. The model from this study, will form the starting point for the present model identification. The model is based on the models used by Nielsen and Madsen (2006) for forecasting of district heating and by Bacher et al. (2012) for forecasting of the heat load in single family houses. These models are based on prior physical knowledge of the heat dynamics, which coupled with statistical time series models creates a grey-box modelling approach. The model selection method used, is a forward selection approach, by first fitting the simplest model without external input from weather forecasts and then add inputs until no clear improvement is found.

The identified model by Bacher et al. (2013), will further on be referred to as *model_{basic}* and is defined as

$$Q_{t+k} = \widehat{Q}_{t+k|t} + \epsilon_{t+k} \quad (4.14)$$

where,

$$\widehat{Q}_{t+k|t} = Q_{wd} + Q_{ra} \quad (4.15)$$

Here Q_{wd} is a diurnal curve, one used for workdays and another for weekends, defined as

$$Q_{wd} = \begin{cases} \delta(t_{tod}, n_{har}, \alpha_{workday}) & \text{for workdays} \\ \delta(t_{tod}, n_{har}, \alpha_{weekend}) & \text{for weekends} \end{cases} \quad (4.16)$$

where $\delta(t_{tod}, n_{har}, \alpha)$ is a harmonic function as described in section 4.1.3. Q_{ra} is the ambient temperature effect divided in two regimes, determined by the opening and closing hours, where 7 to 22 is the opening hours.

The effect is defined as

$$Q_{ra} = \begin{cases} \alpha_{i,open} + \alpha_{a,open} H_a(q) T_{t+k|t}^{a,open} & \text{for opening hours} \\ \alpha_{i,close} + \alpha_{a,close} H_a(q) T_{t+k|t}^{a,close} & \text{for closing hours} \end{cases} \quad (4.17)$$

where $H_a(q) T_{t+k|t}^a$ is the ambient temperature entered through a low pass filter, see section 4.1.1 for further details and $\alpha_{a,open}$ is the coefficient for opening hours and $\alpha_{a,close}$ is the coefficient for the closing hours. The model is fitted

with the k -step recursive least squares scheme described in Section 4.1.2 and the parameters optimized in the model from Bacher et al. (2013) are

- The forgetting factor, λ
- The number of harmonics in the diurnal curve, n_{har}
- The coefficients for input low-pass filters, a_{T_a}

Parameters are optimized in an off-line setting by minimizing the RMSE for each horizon $k = 1, \dots, 42$ separately, as described in 4.1.5. The filtering of the inputs are performed only once for parameter values in a given range, and then used for optimization for all the horizons.

In the model by Bacher et al. (2013) all data available, from November 2011 to November 2012, is used. The period before the November 15th 2011 is used as a burn-in period, which is excluded from the $RMSE_k$ calculation and the large gaps in data is also removed. The local observations are combined with the weather forecasts as described in Section 2.3.

4.2.1 Previous tests

Bacher et al. (2013) carries out a model identification to identify which inputs significantly improves the performance. Solar radiation and wind speed were included in the model, in various combinations, both were let through a low-pass filter, neither one of them improved the forecasting performance. These will therefore not be tested again and the conclusion drawn in the report, is that some non-linear effects in the ambient temperature are not described sufficiently, especially for the longer horizons, where the non-linear effects not included in the model are more clearly seen. This model is very suitable for load forecasting, for supermarket refrigeration, however further improvement can be achieved.

4.2.2 Model evaluation

This basic model is tested with the selected data, described in Section 2.1, for the period from May 1st to August 1st. First the parameters are optimized and afterwards forecasts is conducted for 1-step horizon up to 42-step horizon. The parameters fitted are:

- The forgetting factor, λ

- The coefficients for input low-pass filters, a_{T_a}

The number of harmonics n_{har} is not optimized in this Thesis, $n_{har} = 10$ is chosen, since it otherwise complicates the optimization and causes computational difficulties.

The fitted values for the parameters listed above, is plotted in Figure 4.4 for each horizon k .

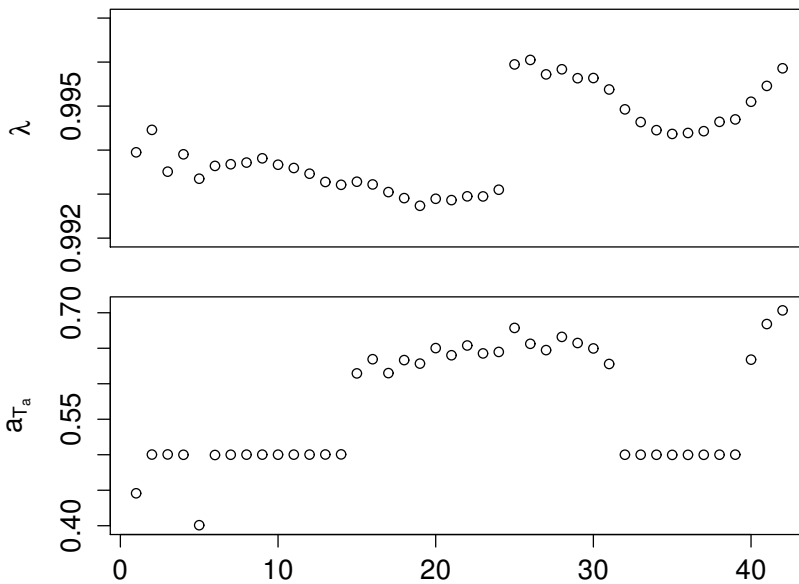


Figure 4.4: The fitted model parameters as a function of horizon k for $model_{basic}$.

The optimized values for λ are between 0.993 and 0.996, which corresponds to a halving time of the weights in the recursive least squares algorithm, from 95 hours (~ 4 days) to 175 hours (~ 7 days) respectively and the coefficient a_{T_a} , for the low-pass filter, varies between 0.401 and 0.703. The forgetting factor shifts to a higher level from horizon 24 to 25 and the pattern in the long horizons are recognized from 2.3, which is discussed later in the Thesis.

The regime splitting done by the model is displayed in the scatter plot in Figure 4.5, opening regime is chosen to be from 7 to 22 and closing regime from 23 to 6, since staff is present in the supermarket, removing the isolation before the

supermarket opens for the customers. It can be seen that some overlap does occur, i.e. some observations from opening hours have a low level compared to the established level of the opening hours, and the other way around, with the majority of observations from opening hours in the low level. It is not possible to completely split in opening and closing hours with no overlap, so this seems to be a good split.

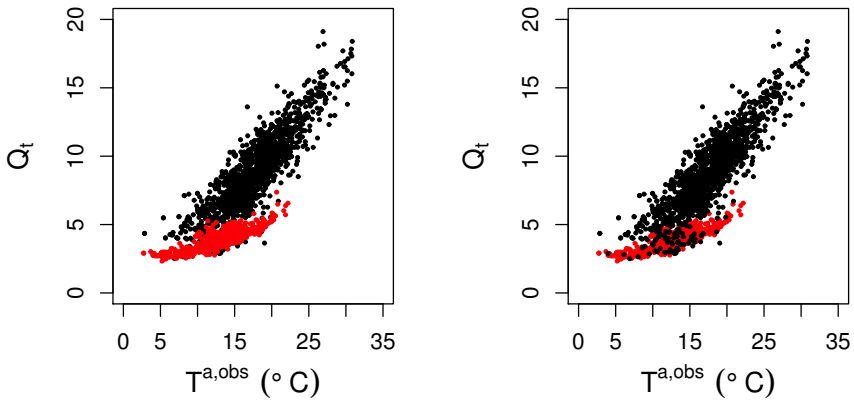


Figure 4.5: Scatter plots of the load versus the ambient temperature, showing the splitting with opening and closing hours. The black points is the opening regime, the red points indicates the closing regime. In the left plot the closing regime is plotted on top of the opening regime and vice versa in the right plot.

The calculated RMSE_k for each horizon is displayed in Figure 4.6. It is noted that the period before the 15th of May 2012 is used as burn-in period, and is therefore excluded from the calculations of RMSE_k .

The RMSE_k has an unusual shift in level from RMSE_{24} to RMSE_{25} . Notice the pattern in the high steps, it is recognized as the pattern discussed in Section 2.3 and is therefore accepted as an effect from external part (DMI) combined with a short period of data (3 months). This also explains the pattern in the fitted parameter λ , seen in Figure 4.4.

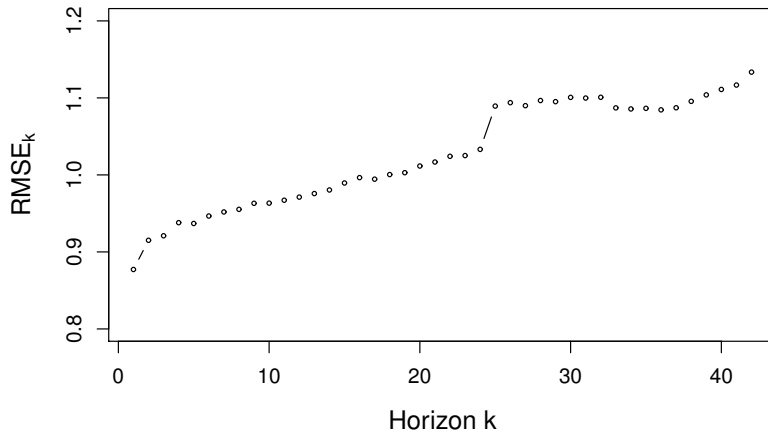


Figure 4.6: RMSE_k for each horizon $k = 1$ to $k = 42$ for model_{basic} .

These RMSE_k are discussed more in Chapter 5.

The model performance is analysed using the residuals together with the RMSE_k . The focus will be on two horizons $k = 1$ and $k = 36$, a short and a longer horizon, this is to give a more manageable overview of the performance. The residuals for horizon $k = 1$ and $k = 36$ are displayed in Figure 4.7, where the same burn-in period used in the calculations of RMSE_k , is excluded from the plot.

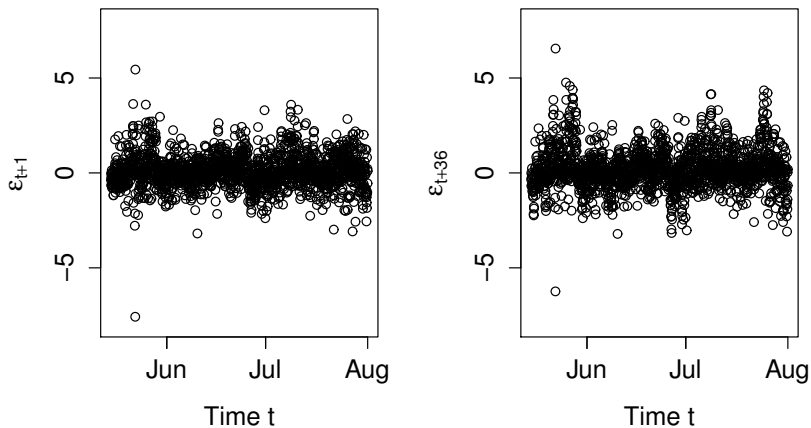


Figure 4.7: Residuals from 1-step ahead predictions (to the left) and 36-step ahead predictions (to the right) for $model_{basic}$.

From this plot it is seen that there is one large residual and another one also a little far from the other residuals. This could be an outlier in the data, which needs to be investigated. Besides from that, there seems to be some weak pattern in the 1-step ahead residuals, which is more clearly seen in the residuals from the 36-step ahead residuals, but they are nicely distributed around zero, which makes them unbiased like white noise.

To investigate the the two large residuals, the forecast and the refrigeration load for a short period from 21st of May to the 22nd of May included, is plotted in Figure 4.8.

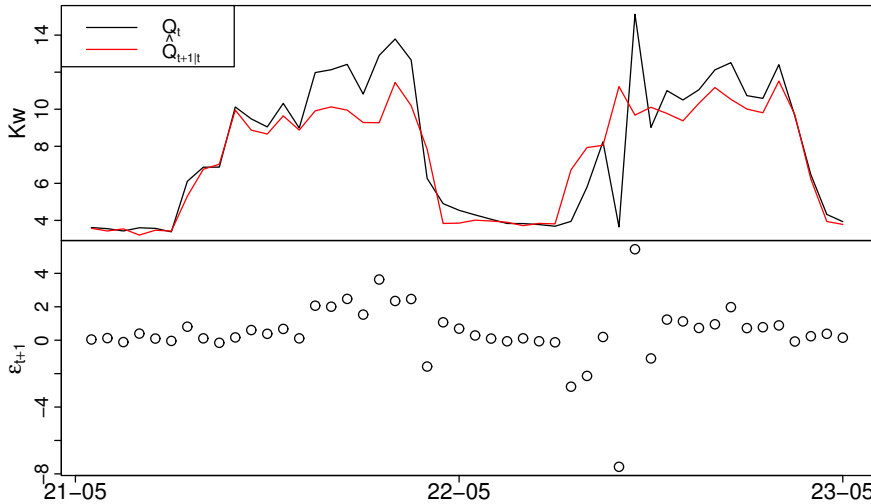


Figure 4.8: First plot shows the 1-step ahead forecast and the refrigeration load for the 21st of May and 22nd of May 2012, bottom plot is the corresponding residuals, for $model_{basic}$.

It is clear that something unusual is happening, with the sudden dive in the morning ramp-up hours, maybe a shut down, or a software issue, mostly leaning towards the shut down for the compressor, due to the high spike in the hour afterwards, which could indicate a need for extra cooling after a shut down. No matter what caused this, it does not look like normal behaviour, so therefore these two residuals is excluded from further analysis. It could be considered excluded from the data before running the model, calculating estimates and making forecast, but when it only concerns two hours, they will not have a significant impact on the fitting and forecast. However, they are disturbing the plots and the residual analysis, and therefore makes it more difficult to spot real patterns and occurrences.

The 1-step residuals and 36-step residuals are plotted in Figure 4.9, without the two excluded values.

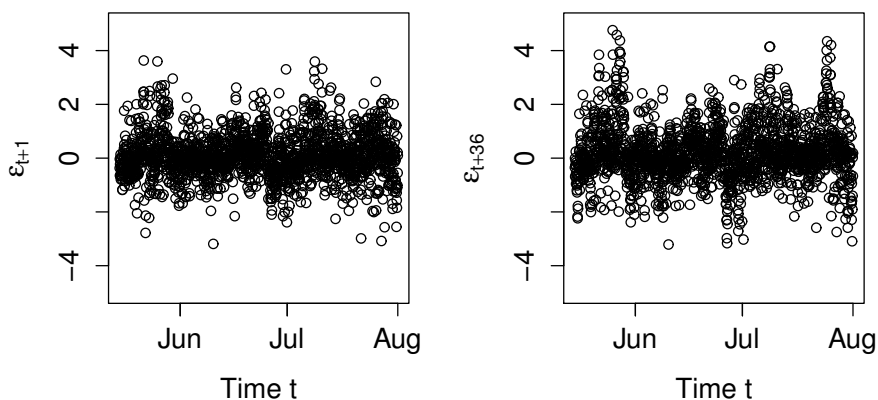


Figure 4.9: Residuals from $model_{basic}$ for 1-step ahead predictions (to the left) and 36-step ahead predictions (to the right) without the two excluded residuals.

Now it is easier to see that there is some pattern in the 1-step ahead residuals and they can not be completely considered as white noise. The 36-step ahead residuals has similar pattern, it is just more clear, which is expected. The ACF is estimated for the 1-step ahead residuals, see 3.1.1 page 20, for further description, which is plotted in Figure 4.10, together with a histogram and QQ-normal plot. The QQ-normal plot is a Quantile-Quantile normal plot, which is a graphical method for comparing the probability distribution for the residuals against a theoretical normal distribution, done by plotting their quantiles against each other.

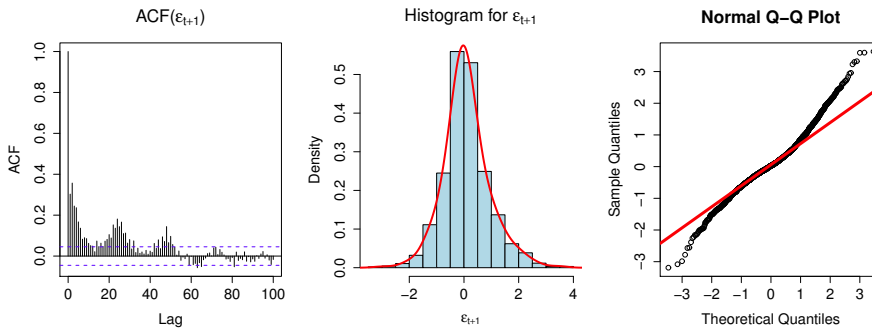


Figure 4.10: The ACF, histogram and QQ-normal plot for the 1-step ahead residuals, for $model_{basic}$.

From the ACF it is clearly seen that some correlations are left for the first lags, also a seasonal pattern around 24 lags is detected. The histogram shows a non-skewed distribution of the residuals, which indicates that the residuals could be normally distributed, the QQ-normal plot, on the other hand, reveals a bit heavy tails compared to the normal distribution. Hence it is found that the residuals are not white noise. Some improvement of the performance can be achieved.

With focus on a shorter period, namely July, the fitted coefficients for the ambient temperature inputs, α_a is plotted in Figure 4.11 for both the opening regime and the closing regime, together with the low-pass filtered ambient temperature input for the 1-step ahead forecast and the corresponding forecast performance.

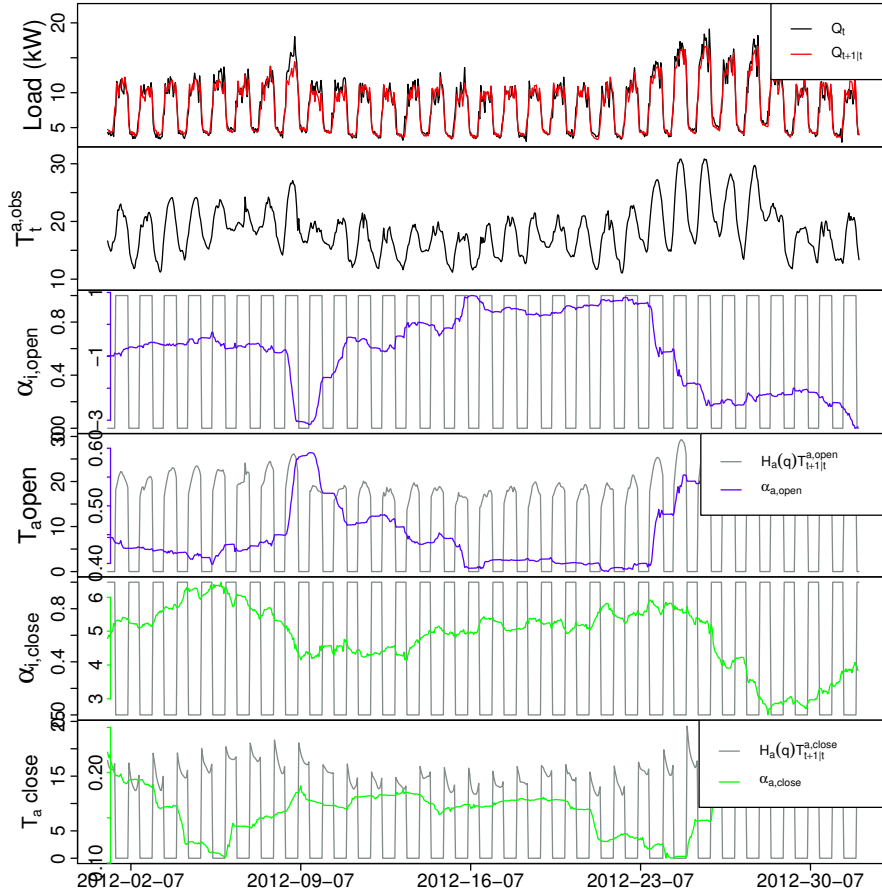


Figure 4.11: First plot is the forecast versus the refrigeration load, next plot is the observed ambient temperature and the last plots is the fitted coefficients for the ambient temperature input, first the intercept and slope for the open regime and the corresponding plots for closing regime, for $model_{basic}$.

These plots display that the coefficient estimates of the inputs varies according to the changes related to the ambient temperature. It is easily seen in the coefficient estimates for the slope α_a , that they increases when there is warm days and decreases again when it gets colder, for example from July 24th and forward, where the temperature is increasing, same is the slope coefficient and the intercept is decreasing. This shows how the model is able to adapt to changing conditions, however the conditions are changing much faster than described by

the model.

The analysis of the residuals is finished with a comparison of the residuals versus the ambient temperature input for 1-step ahead prediction and 36-step ahead predictions. This is plotted in Figure 4.12 where smoothed local kernel regression estimates, calculated with the R-function `loess()`, are added on top as red lines.

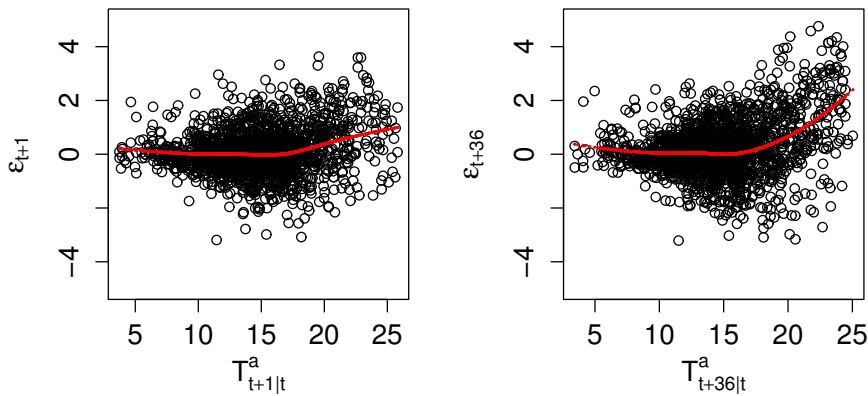


Figure 4.12: 1-step and 36-step ahead residuals versus the predicted ambient temperature used as input, with smoothed local regression estimates as red lines, for $model_{basic}$.

Here it is seen that the conditional mean of the residuals increases with the increase in ambient temperature, and the smoothed estimates shows that the residuals is biased for degrees of the ambient temperature higher than approximately 17°C, it is even more clear in the 36-step residuals. This implies that the model is not describing the non-linear effect from the ambient temperature, sufficiently.

All the discoveries made in this analysis corresponds well to the discoveries made in Bacher et al. (2013), which ensures that the identified model in Bacher et al. (2013) and $model_{basic}$ is the same model. In the following sections, different approaches will be tested, to try an improve the handling of the non-linear effects from the ambient temperature, which is presumed to improve the model performance.

4.3 Basic model with regime from diurnal curve

One way to improve the basic model, can be to divide the ambient temperature into two regimes by use of the diurnal curve, instead of simply the fixed opening and closing hours.

The approach for calculating the diurnal curve used for the regimes, is in an off-line setting, by first running the model with diurnal curve and low-pass filtered ambient temperature, but without regime.

$$Q_{t+k} = \widehat{Q}_{t+k|t} + \epsilon_{t+k} \quad (4.18)$$

$$\widehat{Q}_{t+k|t} = \alpha_i + Q_{wd} + Q_a \quad (4.19)$$

where Q_{wd} is a diurnal curve for weekends and another for workdays, as in Equation (4.16) and $Q_a = H_a(q)T_{t+k|t}^a$, is the effect from the ambient temperature put through a low-pass filter. This diurnal curve with fitted parameters, $\hat{\delta}(t_{tod}, n_{har}, \alpha_{diur})$, is then used for estimating the regime by the sign of the diurnal curve, e.g. negative sign equal night regime and positive, day regime.

The model, $model_{diur}$ is then defined as

$$\widehat{Q}_{t+k|t} = Q_{wd} + Q_{ra} \quad (4.20)$$

Here Q_{wd} is a diurnal curve, as explained in equation (4.16) and Q_{ra} is now defined as

$$Q_{ra} = \begin{cases} \alpha_{i,day} + \alpha_{a,day}H_a(q)T_{t+k|t}^{a,day} & \text{for } \hat{\delta}(t_{tod}, n_{har}, \alpha_{diu}) \geq 0 \\ \alpha_{i,night} + \alpha_{a,night}H_a(q)T_{t+k|t}^{a,night} & \text{for } \hat{\delta}(t_{tod}, n_{har}, \alpha_{diu}) < 0 \end{cases} \quad (4.21)$$

This way of determining the regimes is more dynamic, which makes it possible for the model to adapt to changes in the day and night regime, if e.g. the supermarket changes the opening and closing hours or if they just are different within the week. It gives the splitting of the regimes as displayed in Figure 4.13.

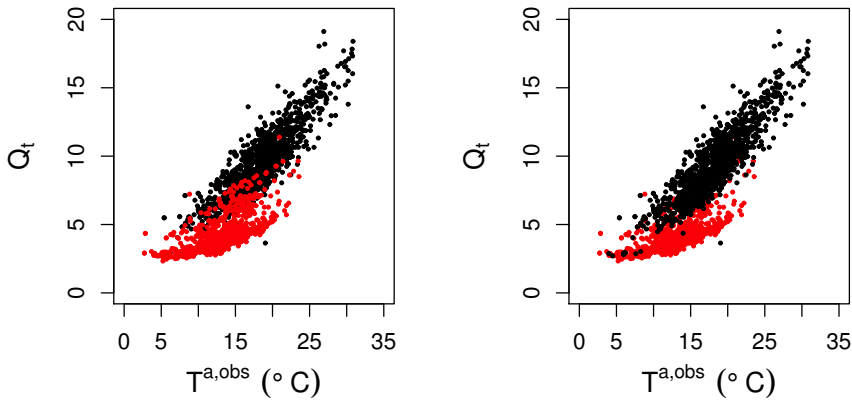


Figure 4.13: Scatter plots of the load versus the ambient, showing the splitting with the diurnal curve. The black points is the positive values indicating day regime, the negative values are the red points indicating the night regime. In the left plot the night regime is plotted in top of the day regime and vice versa in the right plot.

Comparing this to Figure 4.5, an overlap is also occurring here, but unlike the regime split by the fixed opening hours, the majority of the overlap are now from the observations of night regime with high level, i.e. overlapping the day regime. At first glance the splitting from opening and closing hours seems better with fewer overlaps, but maybe the adaptivity will give some advantages.

In the next section the model is evaluated by investigating the fitted parameters and analysing the residuals.

4.3.1 Model evaluation

When evaluating the model, the first thing investigated is the fitted parameters λ and a_{T_a} , which is plotted for each horizon k in Figure 4.14. The parameters is fitted in the same way as mentioned in Section 4.1.5, with the R-function `optim()`.

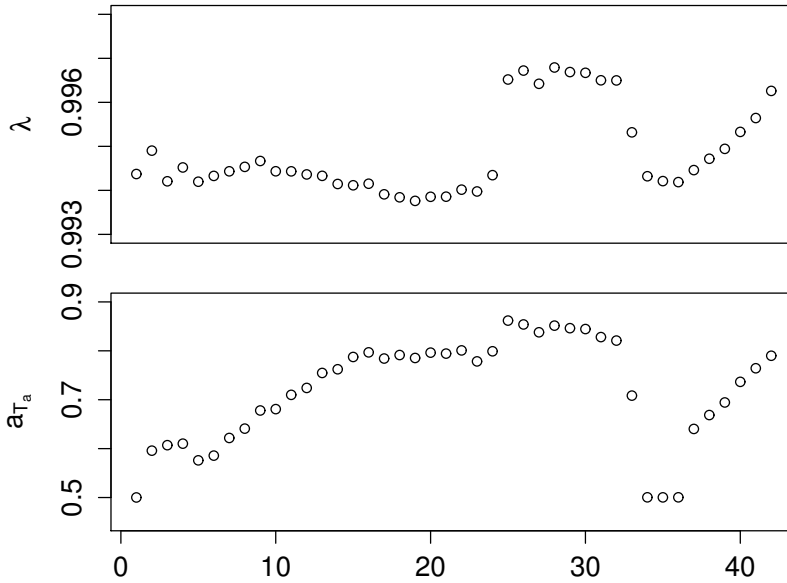


Figure 4.14: The fitted model parameters as a function of horizon k , for $model_{diur}$.

Seen in the plot, the optimized values for λ are between 0.994 and 0.997, which corresponds to a halving time from approximately 110 hours (~ 4.5 days) to 216 hours (~ 9 days) respectively and the coefficient a_{T_a} , for the low-pass filter, varies between 0.500 and 0.862. λ does not change much in the first horizons from $k = 1$ to $k = 24$, then it jumps to another level and stays on that level until $k = 32$ and then drops to approximately the same level as before just to increase again for the rest of the horizons. This pattern is recognized from Section 2.3 page 9, which will be discussed in Chapter 6. The coefficient a_{T_a} increases from $k = 1$ to $k = 33$ and then drops to another level around 0.49, for three horizons, $k = 34$ to $k = 36$, the rest of the horizons are increasing.

The $RMSE_k$ is calculated from the residuals, for each horizon $k = 1$ to $k = 42$ and plotted in Figure 4.15.

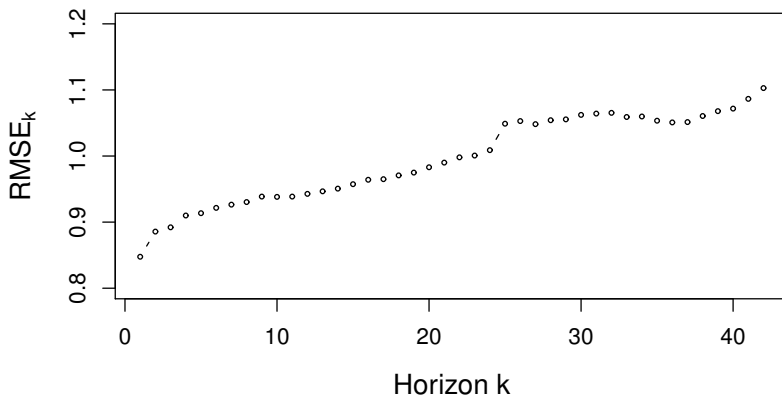


Figure 4.15: $RMSE_k$ for each horizon $k = 1$ to $k = 42$, for $model_{duur}$.

These shows the same pattern as seen for the basic model, with longer horizons performing better than shorter one, which was mentioned earlier in Section 2.3. The $RMSE_k$ will be discussed later, when they are compared with the other models presented in this Thesis.

Now the residuals are analysed, first the same two outliers as detected in Figure 4.7 is removed before investigating the residuals, then the residuals is plotted in Figure 4.16, with 1-step ahead residuals to the left and 36-steps ahead residuals to the right.

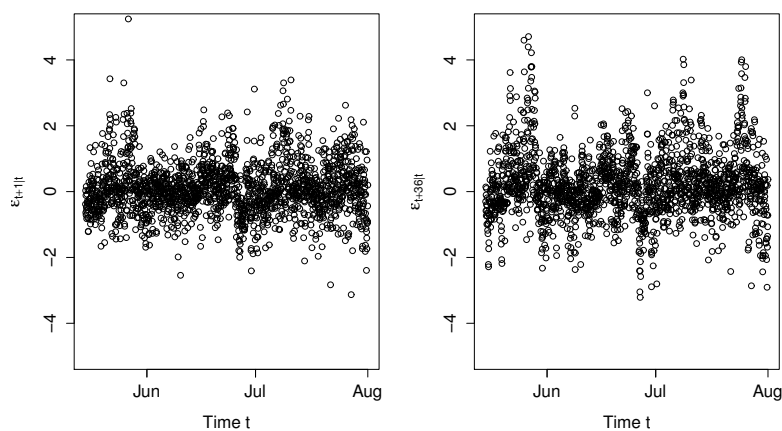


Figure 4.16: Residuals from $model_{diur}$ for, 1-step ahead predictions (to the left) and 36-step ahead predictions (to the right).

For the 1-step ahead residuals it is evenly distributed around zero, with few high residuals. There appears to be a weak pattern in the 1-step ahead residuals, which becomes more clear in the 36-steps ahead residuals, which also was detected in $model_{basic}$. The ACF, histogram and QQ-normal plot are displayed in Figure 4.17, to help with the analysis of white noise properties of the residuals.

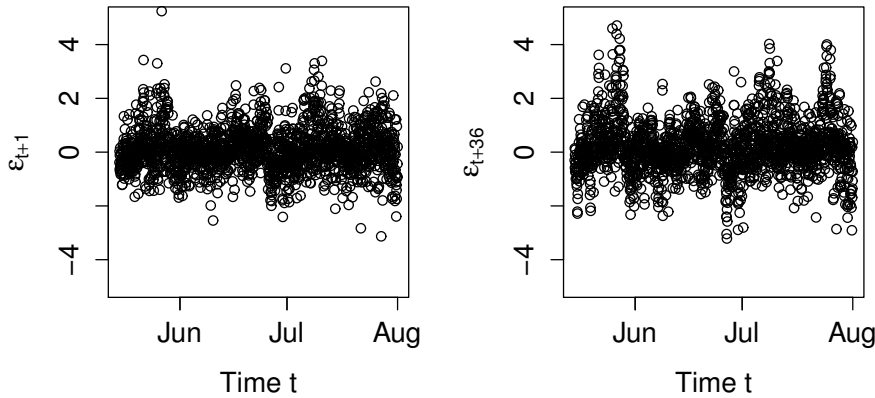


Figure 4.17: The ACF, histogram and QQ-normal plot for the 1-step ahead residuals, for $model_{diur}$.

The ACF plot has correlation at the first lags, approximately until lag 10. The seasonal pattern is more unclear now, which is assumed to be due to a better way of dividing the model in day and night regimes. The histogram has a slightly right-skewed bell shape and much density around zero, this is acceptable for a white noise conclusion. The QQ-normal plot on the other hand still has heavy tails compared to the normal distribution. So still not completely white noise residuals, but a slightly improvement in the seasonal correlation, compared to $model_{basic}$.

The behaviour of the fitted coefficients for the ambient temperature inputs (the slope α_a) are analysed for July. These are plotted in Figure 4.18 together with the forecast, the observed refrigeration load and the observed ambient temperature, all plots is for 1-step ahead horizon, except for the observed ambient temperature.

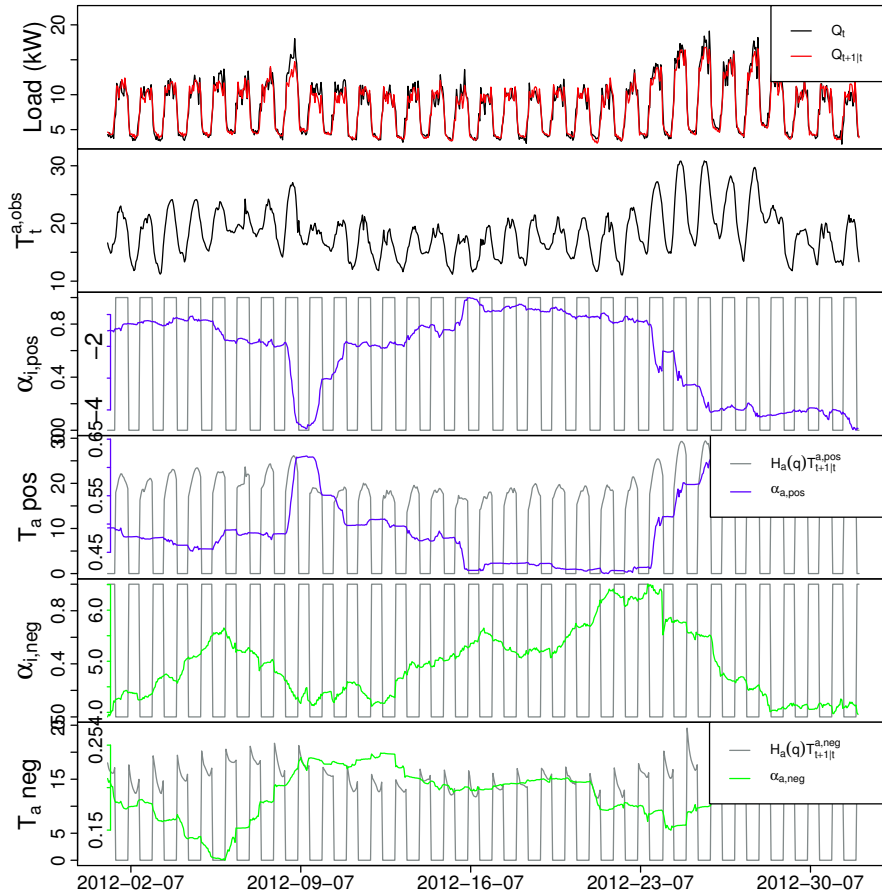


Figure 4.18: First the forecast versus the refrigeration load, next plot is the observed ambient temperature and the last plots is the fitted coefficients for the ambient temperature input, first the intercept and slope for the day regime and the corresponding plots for night regime, for $model_{diur}$.

In this Figure, it is clearly seen that the slope coefficients adapt to changes in the ambient temperature, whenever the temperature goes up, the same does the slope coefficients and when the slope increases, the intercept decreases, indicating the non-linear effect in the ambient temperature. It is easily seen in the day-regime ($\alpha_{a,day}$), but also the night-regime ($\alpha_{a,night}$) reacts to changes in the temperature at night. For example the 8th, there is an increase in the day ambient temperature above 25 °C then the coefficient $\alpha_{a,day}$ increases signifi-

cantly and the day after, the ambient temperature has dropped to under 20 °C, the coefficient also drops, but with a little delay. Which shows that the model is able to adapt to the changing conditions, but since the non-linear effect from the ambient temperature is linear locally in time, it is not able to adapt fast enough.

Clearly, as concluded before, the refrigeration load is highly dependent on the ambient temperature. The residuals is plotted against the 1-step ahead predicted ambient temperature and 36-steps ahead predicted ambient temperature, with `loess` fitted red lines, in Figure 4.19.

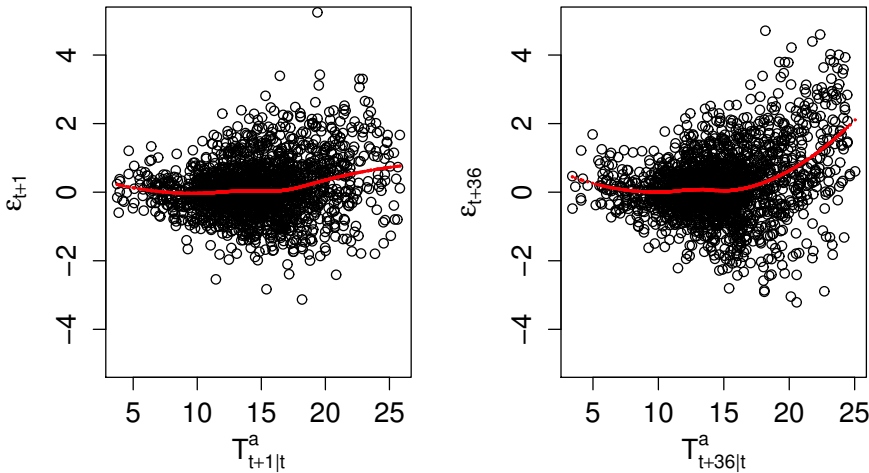


Figure 4.19: 1-step and 36-step ahead residuals versus the predicted ambient temperature used as input, with smoothed local regression estimates as red lines, for *model_{diur}*.

The residuals increases as the ambient temperature increases and the `loess`-fitted red lines shows that the residuals is biased for degrees of the ambient temperature above approximately 17 °C, it is more clear in the 36-step ahead residuals, where the residuals is also slightly biased for degrees of the ambient temperature under approximately 7 °C.

It is expected that this bias is still present, due to the input for the ambient temperature is unchanged compared to the basic model, it is only the method for deciding the regime that has been change. Improvement is found, therefore this way of determining the regimes is kept in the following models.

4.4 Basic model with splines in off-line setting

The main issue in the current model, $model_{diur}$, is the non-linear effect from the ambient temperature, especially above 17 °C, so instead of using the low-pass filtered ambient temperature as direct input, then the low-pass filtered ambient temperature is modelled with a spline function. This is done, to see if this model will react better to the non-linear effect seen between the ambient temperature and the refrigeration load, which was discussed in the evaluation of previous model in Section 4.3.1. With $model_{diur}$ from Section 4.3 as reference, the following model, $model_{sp,off}$ is defined as

$$Q_{t+k} = \widehat{Q}_{t+k|t} + \epsilon_{t+k} \quad (4.22)$$

$$\widehat{Q}_{t+k|t} = Q_{wd} + Q_{rs}^{off} \quad (4.23)$$

where Q_{wd} is the diurnal curve defined in Equation (4.16), and Q_{rs}^{off} is the spline function for the ambient temperature, divided in two regimes in the same way as in $model_{diur}$, with day and night regime from diurnal curve, (4.17). Q_{rs}^{off} is defined as,

$$Q_{rs}^{off} = \begin{cases} \alpha_{i,day} + \alpha_{a,day}(\beta_{i,day} + \sum_j \beta_j^{day} B_{j,p}^{day}) & \text{for } \hat{\delta}(t_{tod}, n_{har}, \alpha_{diu}) \geq 0 \\ \alpha_{i,night} + \alpha_{a,night}(\beta_{i,night} + \sum_j \beta_j^{night} B_{j,p}^{night}) & \text{for } \hat{\delta}(t_{tod}, n_{har}, \alpha_{diu}) < 0 \end{cases} \quad (4.24)$$

with $B_{j,p} = b_{jp} H_a(q) T_{t+k|t}^a$, see Section 4.1.4 for further details.

This model is conducted in an off-line setting, which means that the ambient temperature is estimated with the spline function (Q_{rs}) as input to the model. This estimation of all β_j and β_i are executed with the R-function `lm()`, which is used for linear regression, where the input to this function is the B-spline matrix and the refrigeration load Q_t for the whole period and β_i is the intercept. After that the R-function `predict()` is used to calculate the estimated ambient temperature. This way of implementing splines into the forecast model, is not realistic for an operation of the forecast model, due to the use of observations that is in the future. However, it is an efficient way to see if spline functions can improve the model performance. Only a few degrees of freedom are used and with use of historical data instead, the performance will only be marginally worse.

An important subject to consider, is the choice of order and knots for the spline function. As mentioned in Section 4.1.4, the B-splines is calculated with the use of the R-function `bs()`, in this function it is possible to specify the order p as `degree` and then there is two options for choosing the knots together with the degree. Either they can be specified via a degrees-of-freedom argument `df`, which is an integer, or via a knots argument `knots`, which is a vector giving

the desired placements of the knots. If the degrees-of-freedom argument is used then the knots is selected based on quantiles of the data input, in this case the ambient temperature. There is also the choice of adding an intercept. An example is given below.

EXAMPLE 4.2 (KNOTS SELECTION IN THE R-FUNCTION BS())

If `bs(x, degree=2,df=5)` is called, then the basis includes:

- *2 boundary knots - default at minimum and maximum of x*
- *3 interior knots (`df-degree`) - placed at quantile 25%, 50% and 75%*

in total 5 knots. This will give five B-spline functions (interior knots + degree).

The question is now, what is a good choice of degree and knots? This depends on what the spline function should be able to do and on the data it is fitted on. A good rule of thumb is to have the spline function obtain a curve estimate that does not display too many fluctuations., which can not be seen in the data. Two examples are given in Figure 4.20, containing the 1-step ahead predicted ambient temperature T_{t+1}^a versus the refrigeration load Q_t from the day regime, with what could be concluded as, a good choice (to the left) and a bad choice (to the right).

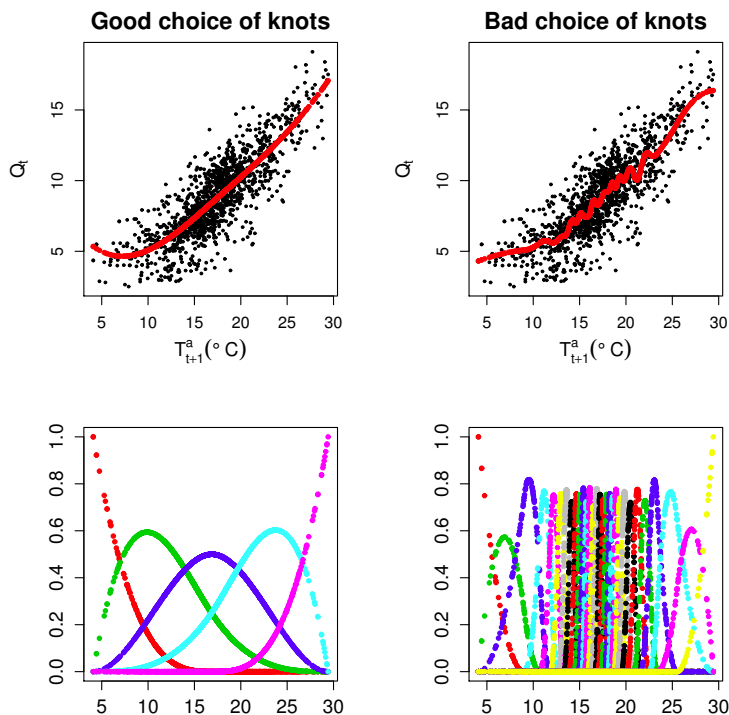


Figure 4.20: Examples of a good choice of knots (to the left) and a bad choice of knots (to the right).

In $model_{sp,off}$, `degree` is chosen to be 3 and `df` is 5, for both the day regime and night regime, made for the 1-step predicted ambient temperature. The intercept is chosen to be included by `lm()` when the coefficients are estimated and not included in the B-splines, it is possible to do it with intercept from B-spline and no intercept from `lm()` and it will not give completely the same result, but the difference in the final spline fitted ambient temperature is marginal. The calculated B-splines are displayed in Figure 4.21.

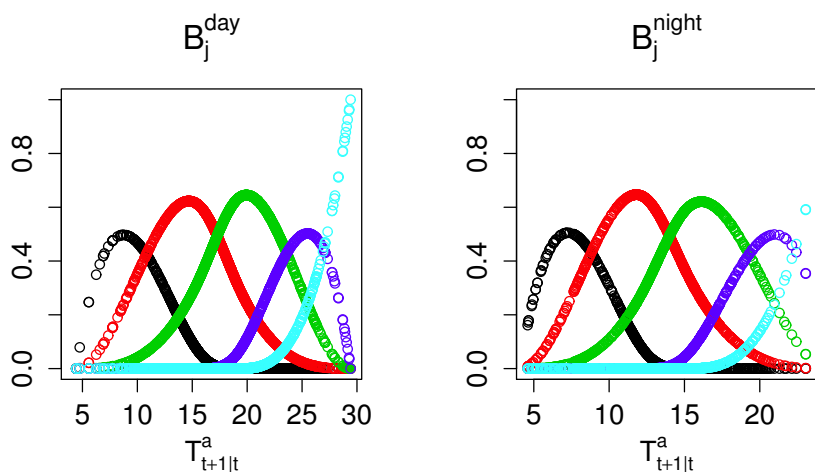


Figure 4.21: The B-splines used as input for 1-step prediction plotted against the low-pass filtered ambient temperature input, divided in the day and night regime, for $model_{sp,off}$.

In this model it is not taken into consideration, if other choices of knots are better for other k -step predicted ambient temperatures, because the k -step predicted ambient temperature are not far from each other and will therefore not effect the spline function sufficiently. The same choice is used for each k -step, $k = 1, \dots, 42$, since it is found to be a good choice.

In the next section the model performance and properties are evaluated.

4.4.1 Model evaluation

Before analysing the residuals, the fitted coefficients, forgetting factor λ and the input coefficient for the low-pass filter a_{T_c} , is analysed in Figure 4.22.

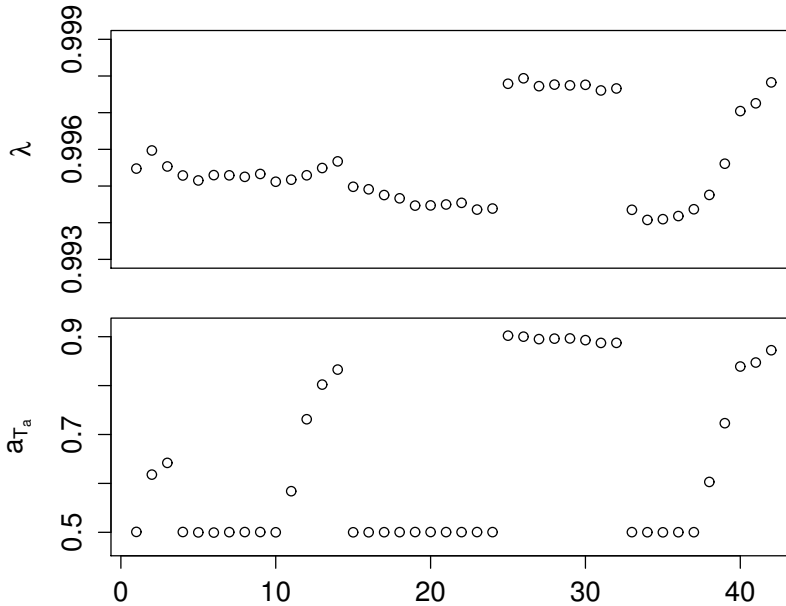


Figure 4.22: The fitted model parameters as a function of horizon k , for $model_{sp,off}$.

The optimized values for the forgetting factor λ are varying between 0.994 and 0.998, which gives a halving time of approximately 117 hours (~ 5 days) to 336 hours (~ 14 days). It is decreasing a little from $k = 1$ to $k = 24$, then it jumps to a level around 0.998 for the next eight horizons, $k = 25, \dots, 32$ and drops again, for increasing in the end towards $k = 42$. This pattern is recognized from previous and will be discussed in Chapter 6. The input coefficient for the low-pass filter is fluctuating between 0.499 and 0.902. This is a relatively large range and large parts of the horizons for the low-pass filtered input are staying at a value close to 0.5, this behaviour should be investigated in future work.

The forecast performance is measured by calculating the $RMSE_k$ (from Equation (2.3)) for each horizon k , these are plotted in Figure 4.23.

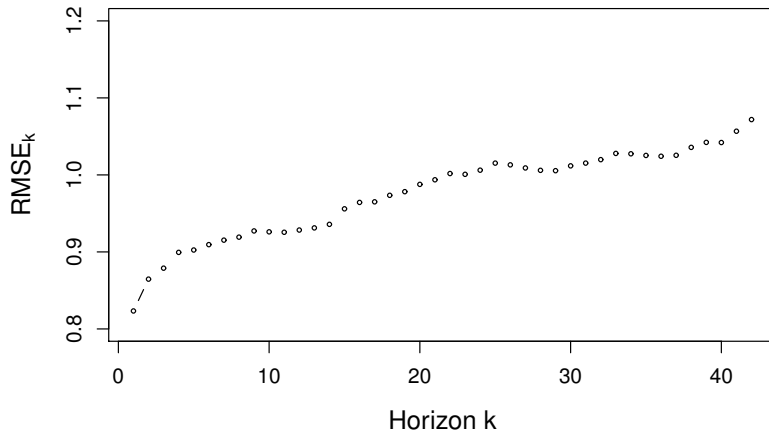


Figure 4.23: The $RMSE_k$ for each horizon k , for $model_{sp,off}$.

The jump in the RMSE from $k = 24$ to $k = 25$ seen in $model_{basic}$ and $model_{diur}$ is not present in this model. But there is still some pattern with the $RMSE_k$ decreasing from $k = 26$ to $k = 30$, this is a very small decrease, which presumably is caused by the predicted ambient temperature from DMI, seen in 2.3. The $RMSE_k$ s for this model is compared with the other models in Chapter 5.

The model is evaluated by a residual analysis carried out in the following. The residuals for horizon $k = 1$ and $k = 36$ is plotted in Figure 4.24 and the same outliers as mentioned in the evaluation of $model_{basic}$ are removed from the residual analysis.

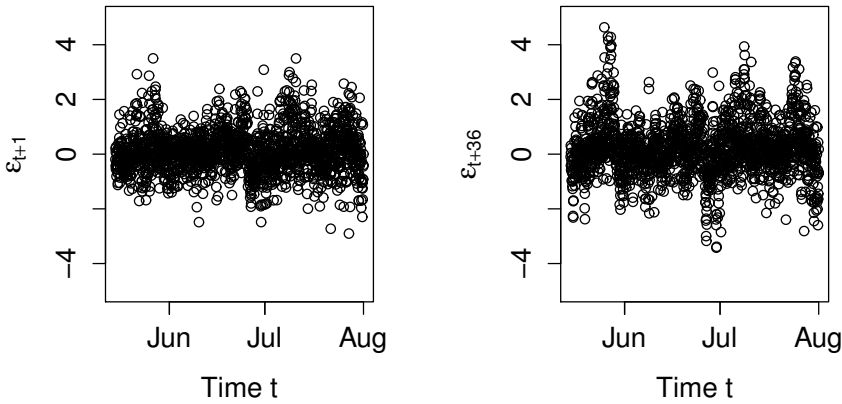


Figure 4.24: The residuals for horizon $k = 1$ (to the left) and $k = 36$ (to the right), for $model_{sp,off}$.

The residuals for horizon $k = 1$ is nicely spread around zero, though a small curving pattern is faintly showing, which is more clear in the residuals for horizon $k = 36$, but for $k = 1$ it is very close to being unbiased like white noise. To investigate the residuals further, the ACF, histogram and QQ-normal plot is displayed in Figure 4.25, for horizon $k = 1$.

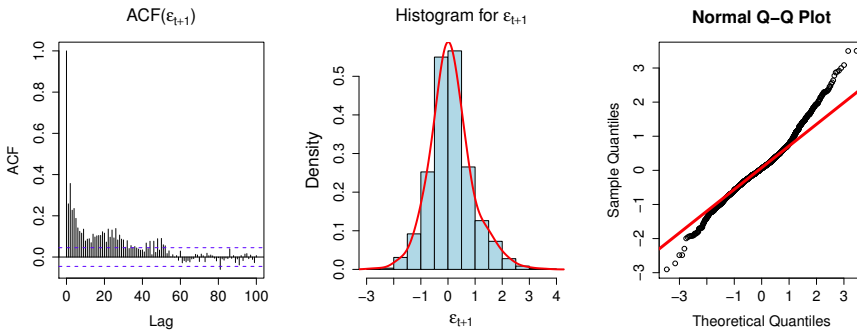


Figure 4.25: The ACF, histogram and QQ-normal plot for the 1-step ahead residuals, for $model_{sp,off}$.

In the ACF plot correlation are seen in the first lags, which is decaying quickly.

There is a small wavy pattern, which is decaying. The histogram has a non-skewed bell, which could indicate normal distributed residuals (white noise). The QQ-normal plot is closer to being on a straight line, than seen in the two earlier models, but still with some heavy tails. The residuals looks more satisfying, but also kept in mind that there is used informations that would not be available in practice.

With focus on July, the fitted coefficients for the spline functions, modelled on the low-pass filtered ambient temperature is plotted in Figure 4.26, together with the forecast, refrigeration load and the observed temperature, with the purpose of analysing the behaviour of the coefficients.

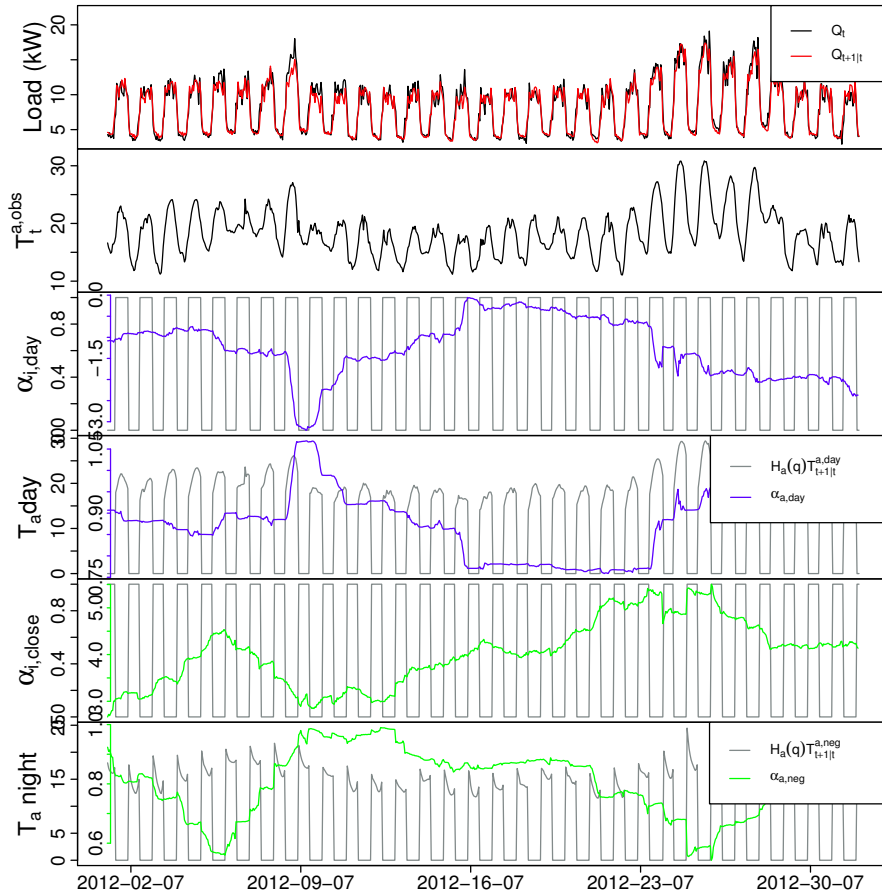


Figure 4.26: First plot shows the forecast versus the refrigeration load, next plot is the observed ambient temperature and the last plots is the fitted coefficients for the ambient temperature input, both the intercept and the slope for the day and night regimes, for $model_{sp,off}$.

From this plot it is seen that the slope coefficient is adapting to changes in the ambient temperature. It is more clear in the day-regime (diurnal positive), due to the more varying temperatures. The intercepts are changing opposite of the slope, which is expected. If the spline input describes the non-linear effect perfectly, the slope coefficient would be constantly 1, it is seen that the coefficient values for the slope have increased so they are closer to 1, which indicates that the spline fitted ambient temperature is describing the non-linear effect better

than $model_{dir}$.

To see if the model is handling the non-linear effects from the ambient temperature sufficiently, a plot of the residuals versus the predicted ambient temperature for 1-step horizon and 36-step horizon, with `loess` fitted red lines, are displayed in Figure 4.27.

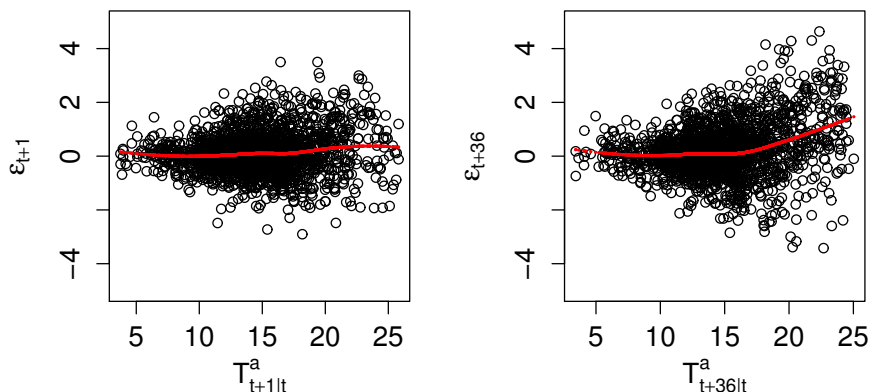


Figure 4.27: 1-step prediction errors and 36-step prediction errors with loess fitted red lines, for $model_{sp,off}$.

The conditional mean of the residuals is increasing as the ambient temperature is increasing, the bias seen in the previous models is lesser for the 1-step predictions, the 36-steps predictions are still slightly biased for degrees above 17°C. The improvements in the residuals, encourage to implement the splines, without using unknown refrigeration load.

4.5 Basic model with splines in on-line setting

As mentioned before in Section 4.4, the off-line method for implementing splines is a bit optimistic, since data from the whole period is used. A way to outcome this is to input the B-splines directly into the model, i.e. by adding them to the regressor vector, described in Section 4.1.2, so it becomes recursively and is not created on unknown observations. This method of implementing splines is

in on-line setting and is defined as $model_{sp,on}$;

$$Q_{t+k} = \widehat{Q}_{t+k|t} + \epsilon_{t+k} \quad (4.25)$$

$$\widehat{Q}_{t+k|t} = Q_{wd} + Q_{rs}^{on} \quad (4.26)$$

with Q_{wd} still being the same diurnal curve as defined in Equation (4.16) and Q_{rs}^{on} is the B-splines for the low-pass filtered ambient temperature input, divided in the regimes; day and night regime as defined in $model_{diur}$.

Q_{rs}^{on} is defined as

$$\widehat{Q}_{rs}^{on} = \begin{cases} \alpha_{i,day} + \beta_{i,day} B_{int,p}^{day} + \sum_j \beta_j^{day} B_{j,p}^{day} & \text{for } \widehat{\delta}(t_{tod}, n_{har}, \alpha_{diu}) \geq 0 \\ \alpha_{i,night} + \beta_{i,night} B_{int,p}^{night} + \sum_j \beta_j^{night} B_{j,p}^{night} & \text{for } \widehat{\delta}(t_{tod}, n_{har}, \alpha_{diu}) < 0 \end{cases} \quad (4.27)$$

with $B_{j,p} = b_{jp} H_a(q) T_{t+k|t}^a$, see Section 4.1.4 and $n_{har} = 10$. The knots choice is the same as in the previous model, $model_{sp,off}$, which was **degree**=3 and **df**=5 and $B_{int,p}$ is the B-spline for an intercept. In Figure 4.28 the B-spline input for 1-step ahead prediction is displayed, plotted against the low-pass filtered ambient temperature input.

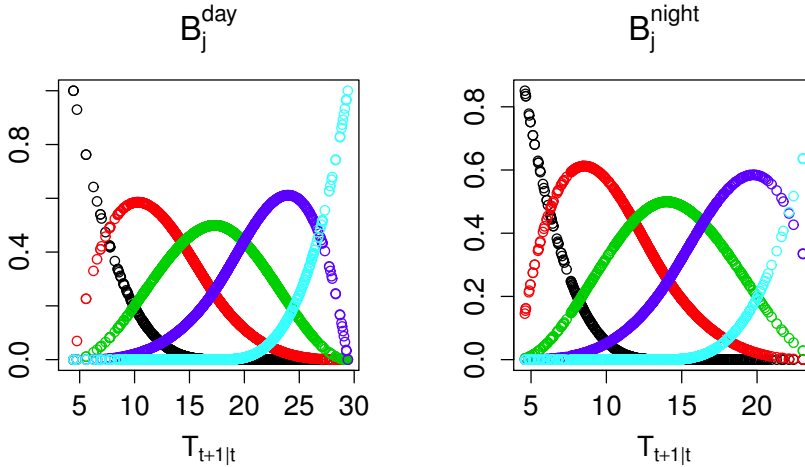


Figure 4.28: The B-splines used as input for 1-step prediction plotted against the low-pass filtered ambient temperature input, divided in the day and night regime, for $model_{sp,on}$.

It is expected that this model will perform slightly worse than $model_{sp,off}$, because of the missing information from the refrigeration load, though it will be a more realistic model, to use.

4.5.1 Model evaluation

In this section the model is evaluated, by looking at the fitted model parameters, the $RMSE_k$ of the prediction errors and a residual analysis is conducted.

First the fitted model parameters is displayed in Figure 4.29, which is obtained from the R-function `optim()` as described in Section 4.1.5. Due to some computational difficulties, with the optimization algorithm hitting some values making a matrix in RLS singular, some programming has been done so that `optim()` skips these.

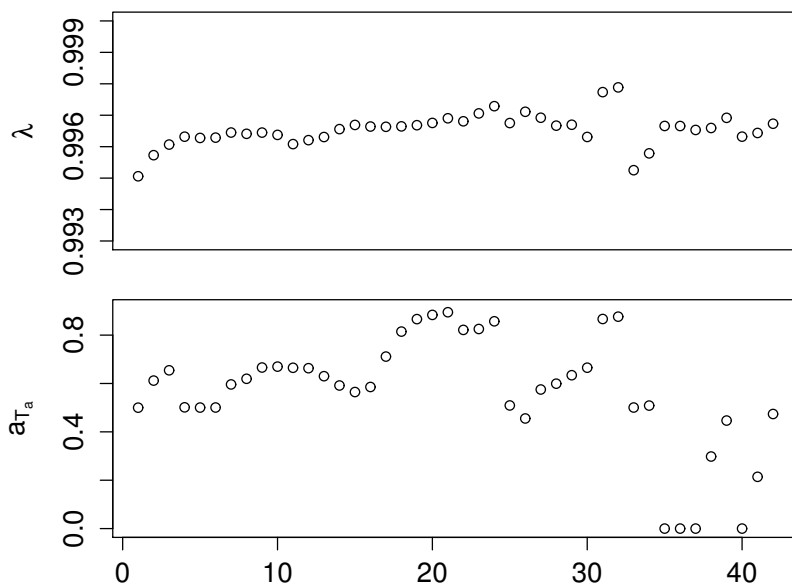


Figure 4.29: The fitted model parameters as a function of horizon k , for $model_{sp,on}$.

The optimized forgetting factor λ is varying between 0.995 and 0.998, which gives a halving time of approximately 140 hours (~ 6 days) to 327 hours (~ 14 days). The forgetting factor is increasing a little in the beginning, then it is staying stable around 0.996 until $k = 30$, then it is fluctuating a little, thus to become stable again around the 0.996. The coefficient for the low-pass filter is fluctuating a lot, especially in long horizons. The impact from this coefficient is not as significant as in $model_{basic}$ and $model_{diur}$, due to low-pass filtered ambi-

ent temperature is only used for calculating the splines, which are not changing drastically for different filtered ambient temperatures.

The forecast performance is measured by the $RMSE_k$, which is calculated for horizon $k = 1$ to $k = 42$ with Equation (2.3) and plotted in Figure 4.30.

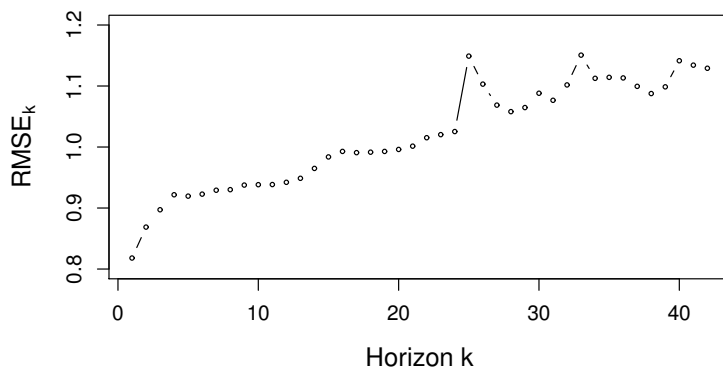


Figure 4.30: The $RMSE_k$ for each horizon k , for $model_{sp,on}$.

The $RMSE_k$ is increasing slightly from $k = 1$ to $k = 24$, a large jump from $k = 24$ to $k = 25$ is seen and then it is fluctuating a little with a slight increase for $k = 26$ to $k = 42$. Further discussion and evaluation is conducted in Chapter 5, where it will be compared to the other models in this thesis.

The residual analysis is the next thing investigated, first the residuals for a short horizon $k = 1$ and a long horizon $k = 36$ is plotted in Figure 4.31

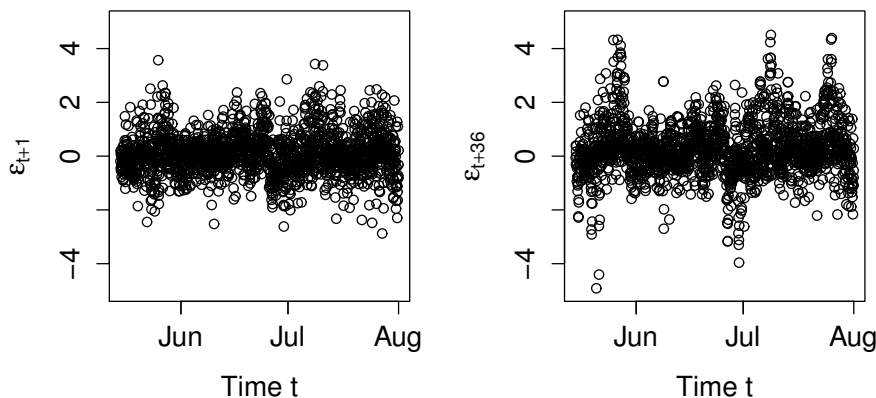


Figure 4.31: The residuals for horizon $k = 1$ (to the left) and $k = 36$ (to the right), for $model_{sp,on}$.

From these plots it is seen that the residuals is nicely distributed around zero, but weak pattern is detected in the 1-step residuals, which is more clear in the 36-steps residuals. So from this it can not be concluded that the residuals is unbiased like white noise, but it is not far from. To investigate this further the ACF, histogram and QQ-normal plot is displayed in Figure 4.32.

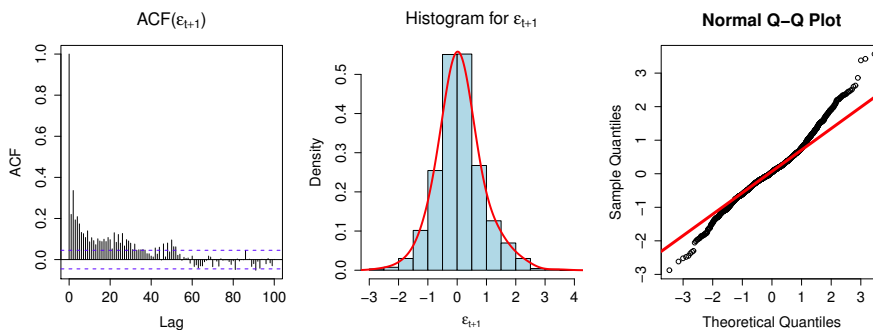


Figure 4.32: The ACF, histogram and QQ-normal plot for the 1-step ahead residuals, for $model_{sp,on}$.

The ACF plot here shows correlation in the first approximately 30 lags, the wavy

pattern seen in the previous models is more unclear. The histogram shows a non-skewed bell, which indicates that the residuals is close to white noise. The QQ-normal plots has heavy tails, but compared to $model_{basic}$ and $model_{diur}$ there is a small improvement. The coefficients for the B-splines for July is investigated in Figure 4.33.

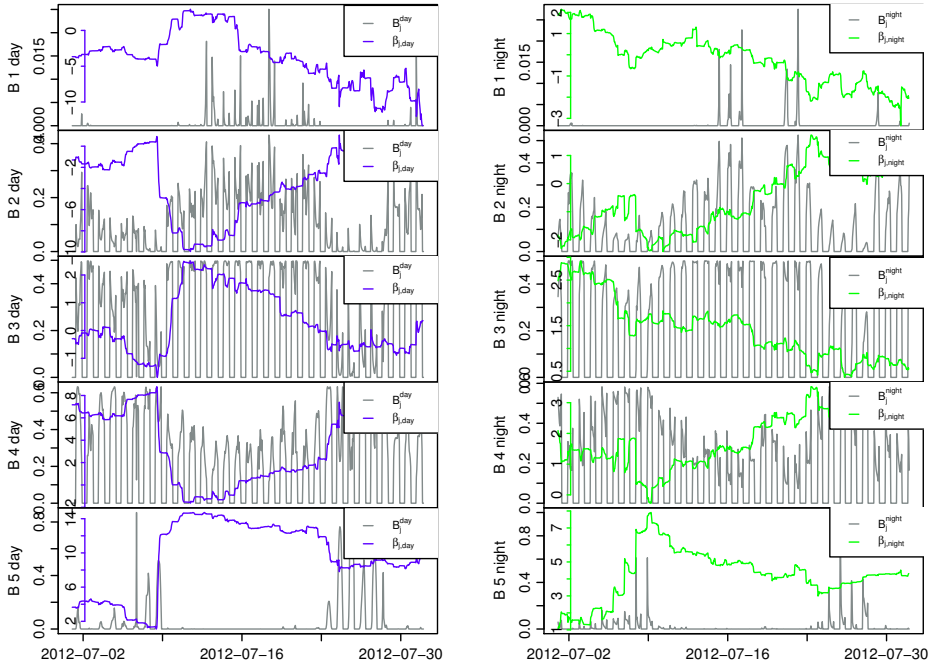


Figure 4.33: Plots of each coefficients for the B-splines, in the day and night regime respectively, the first in each column, the B-spline B_1 day and B_1 night corresponds to the B-spline β_i for the intercept, together with the B-spline inputs, for $model_{sp,on}$.

The coefficient estimates have very high values, either positive or negative, compared to the other models, which is due to the B-spline inputs are of value between 0 and 1. It is seen that the coefficients are fluctuating in a relatively large range, which were not expected, they should be more stable, if they should be able to describe the non-linear effect from the ambient temperature sufficiently. The sudden change in the coefficient values around 8th of July, seems like they are learning from the high ambient temperatures for the first time. To make the coefficients more stable, fitting with more data could be worth trying.

The last analysis of the residuals is displayed in Figure 4.34, which is a plot of 1-step residuals versus 1-step predicted ambient temperature with a smoothed local kernel regression estimates calculated with the R-function `loess()`, added as a red line and a corresponding plot for horizon $k = 36$. It is for the period from 15th of May to 1st of August.

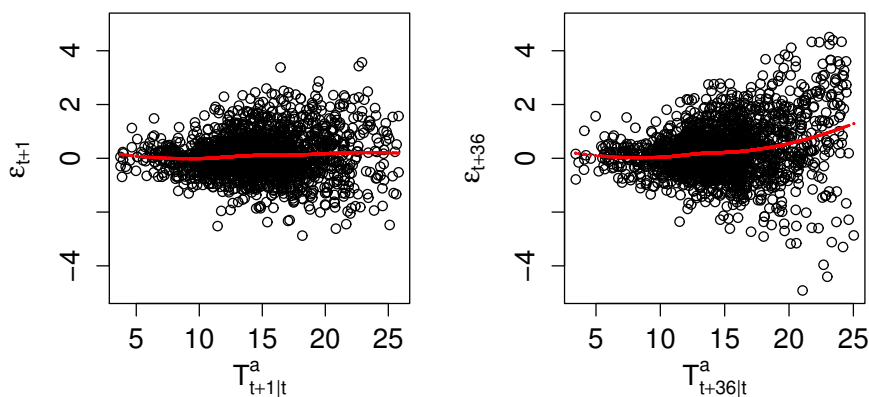


Figure 4.34: 1-step residuals and 36-step residuals versus the ambient temperature input with loess fitted red lines, for $model_{sp,on}$.

The plots reveals that the conditional mean of the residuals increases with the ambient temperature. When comparing to $model_{basic}$ it is less increasing and less spread out. The smoothed estimation shows almost a straight line for the 1-step horizon plot, which means that the bias seen in the other models is removed, the residuals are still biased in the high horizons ($k = 36$), but slope of the red line has decreased significantly. This indicates that this model, $model_{sp,on}$ is describing the non-linear effect from the ambient temperature better than all the other models, but the peaks in the $RMSE_k$ is showing otherwise.

It can be concluded that there is some non-linear effect to recover from the spline functions, but if the forecasting performance is better will be discussed in the next Chapter, where all model performance is compared and evaluated.

Results

In this chapter the forecast results from the five different models, described and evaluated in this Thesis, are compared and analysed. The four models, described in Chapter 4, the $model_{basic}$, $model_{diur}$, $model_{sp,off}$ and $model_{sp,on}$, are analysed by calculating the $RMSE_k$, see Equation (2.3), for 42 horizons, $\{k = 1, \dots, 42\}$.

The performance of the model presented in Chapter 3, $ARIMA_{(3,1,1) \times (1,1,1)}$, is calculated as $RMSE_1$ for 1-step ahead residuals, which is compared to the other models by the $RMSE_1$, which is listed in Table 5.1 for each model.

Table 5.1: The $RMSE_1$ per model.

Model	$RMSE_1$
$ARIMA_{(3,1,1) \times (1,1,1)}$	1.0125
$Model_{basic}$	0.8772
$Model_{diur}$	0.8476
$Model_{sp,off}$	0.8233
$Model_{sp,on}$	0.8181

It is clearly seen that the ARIMA-model performs worse than the adaptive linear time-series models, due to the higher $RMSE_1$ value. Considering the refrigeration load having a range from approximately 2 kW to 19 kW, then a $RMSE_1$

of 1.0125 is not a bad performance, but $model_{basic}$ performs significantly better with approximately 13% improvement and at the same time, recalling from Section 3.3, the performance of the ARIMA-model is not good for long horizons. Hence it is concluded that a simple linear ARIMA-model is not forecasting refrigeration load sufficiently, thus it should not be preferred over the other models and it is therefore not considered in the remaining analysis.

With the ARIMA-model out of the picture, the adaptive linear time-series models are compared by each horizons ($k = 1, \dots, 42$), displayed in Figure 5.1.

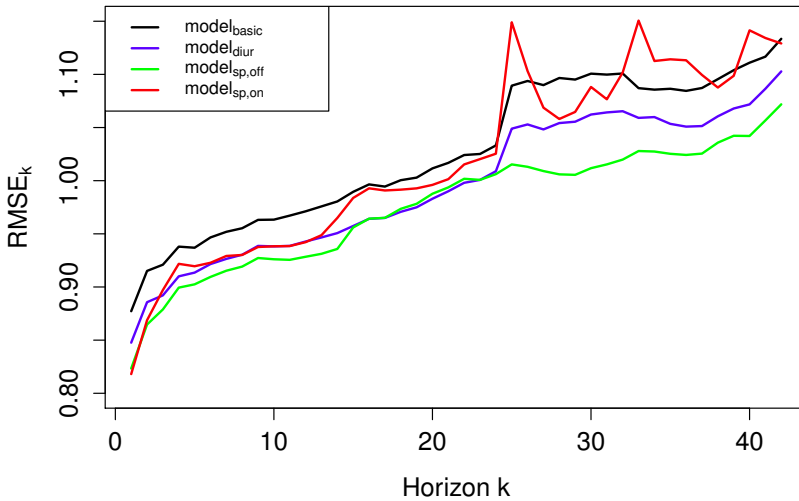


Figure 5.1: Plot of the $RMSE_k$ from each model, for horizon $\{k = 1, \dots, 42\}$.

From this it is clearly seen that there is a significant improvement in the forecasting performance from $model_{basic}$ to $model_{diur}$, so no doubt that the regime splitting from the diurnal curve is better in this case, maybe it is a coincidence and tested on more data might give another conclusion. Nevertheless the diurnal curve is a more dynamic method and is able to adapt to different opening and closing hours, which makes to model usable for other supermarkets than this Fakta.

As found in the previous chapter, $model_{basic}$, $model_{diur}$ and $model_{sp,on}$ have a jump in the $RMSE_k$ from $k = 24$ to $k = 25$, the same jump is not present in $model_{sp,off}$, which is investigated further in Chapter 6

When comparing $model_{diur}$ with $model_{sp,off}$, there is improvement in the first horizons from $k = 1$ to $k = 14$, then up to $k = 24$ the performance is approx-

imately equal, for then again being better. The performance from $model_{sp,off}$ is a bit optimistic, due to the use of all observations for the period modelled, but only a few degrees of freedom are used. In the long horizons around $k = 36$ the same pattern as mentioned in Section 2.3 is not showing here, but it is showing just right after horizon $k = 25$, where the performance for $k = 26$ is better than the previous one. To investigate if this is a coincidence or if it is just better in those horizons, the model should be modelled on a larger set of data. This is presumably caused by the pattern mentioned before in Section 2.3.

The last performance to evaluate, is for $model_{sp,on}$, comparing this with $model_{diur}$, $model_{sp,on}$ is performing better in horizon $k = 1$ and $k = 2$ and are worse the rest of the horizons. Some unusual large spikes are detected in horizon $k = 25$ and $k = 33$, these are discussed further in Chapter 6.

Beside from the spikes, the pattern is close to follow the pattern of $model_{sp,off}$, which makes sense because the B-splines are modelled in the same way, it was also expected that $model_{sp,off}$ would perform better than $model_{sp,on}$, due to the use of unknown refrigeration load in $model_{sp,off}$.

Even though $model_{sp,on}$ is performing worse than $model_{diur}$, there are still some non-linear effect from the ambient temperature that is explained better, see Figure 4.34 in Chapter 4, which is worth investigating further.

The results presented in this chapter are discussed in Chapter 6, together with future work for refrigeration load forecasting models.

Discussion

From the results presented in the previous chapter it is found that the methods used for $model_{basic}$, $model_{diur}$, $model_{sp,off}$ and $model_{sp,on}$ are all suitable for refrigeration load forecasting, and the $ARIMA_{(3,1,1) \times (1,1,1)}$ was found inadequate, the model is therefore not discussed further. In this chapter the models and results are discussed and suggestions for further improvement are presented.

The jump seen in the $RMSE_k$ from $k = 24$ to $k = 25$, for $model_{basic}$, $model_{diur}$ and $model_{sp,on}$, but not for $model_{sp,off}$, is interesting and therefore investigated further. Looking at the different inputs for the models, it is found that the diurnal input is the cause of this jump, which is displayed in Figure 6.1, where the diurnal input for $k = 24$ and $k = 25$ from $model_{diur}$, is plotted together with the observed refrigeration load, predicted refrigeration load and the corresponding residuals for the period 19th to 27th of May.

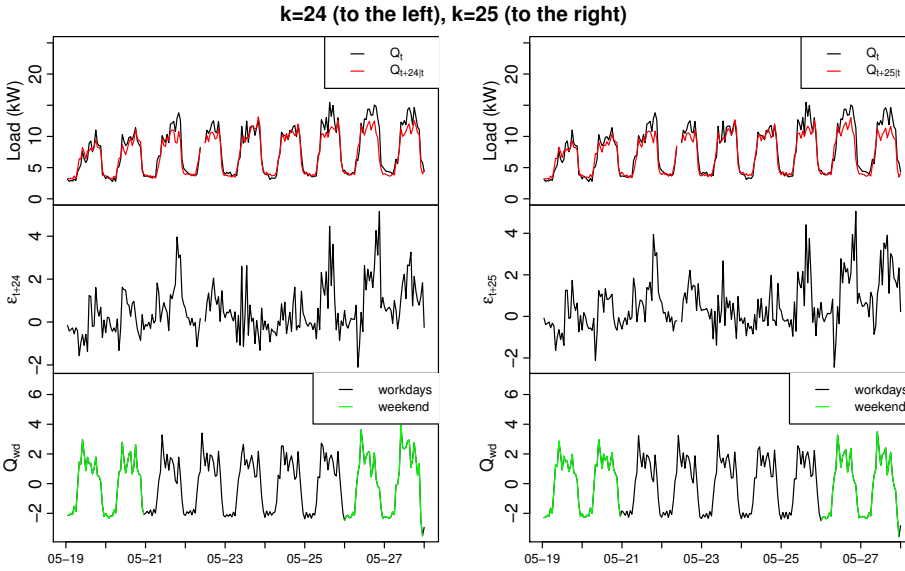


Figure 6.1: Plot of the observed and the predicted refrigeration load, for $k = 24$ and $k = 25$, together with the corresponding residuals and diurnal input, in period 19th to 27th of May for $model_{diur}$.

When looking at the last day, Sunday May 27th, it is clearly seen that for $k = 24$ the diurnal is responding to the errors from the days before, by increasing the coefficients, which changes the diurnal input. For $k = 25$ there is almost no respond to the error, the diurnal input from the day before, a Saturday, is almost the same. This is presumable due to the daily pattern in the data and $model_{sp,off}$ is describing the ambient temperature from the splines better, which makes the errors smaller and therefore less need for the diurnal input to change, this makes the difference between $k = 24$ and $k = 25$ smaller. This behaviour is also seen in the forgetting factor λ , which is having the same jump from $k = 24$ to $k = 25$. The behaviour of the diurnal curve could be investigated further to improve the diurnal curve input.

Considering the $RMSE_k$ only, $model_{sp,off}$ is the best model, but because of the fact, that there have been used data, which in principle are not available at the time t , where the forecasts are calculated, the result is a bit optimistic. It is not possible to implement this model operationally, however using only historical data from previous years, it is presumed that nearly the same performance can be achieved, since the non-linearity of the system most likely changes very slow.

The second best model, when looking at the RMSE_k is model_{diur} , in the very short horizon ($k = 1, 2$) $\text{model}_{sp,on}$ is better than model_{diur} , but in the longer horizons from $k = 13$ to $k = 42$, model_{diur} are performing best. Even though model_{diur} are better for the majority of horizons, the RMSE_k are only in average 3% lower than $\text{model}_{sp,on}$ for horizon $\{k = 13, \dots, 42\}$, which might not seem as a significant improvement, but considering the average magnitude of the residuals for $\text{model}_{sp,on}$ are between 0.82 and 1.15, compared to refrigeration load being between 2.3 kW and 19.1 kW, the residuals are small and therefore more difficult to reduce, so therefore model_{diur} are a somewhat significant better model than $\text{model}_{sp,on}$. Even though $\text{model}_{sp,on}$ 1-step prediction residuals shows almost white noise, it seems to be unstable and over-parametrized, considering the peaks in the RMSE_k and further development must be carried out.

The RMSE_k are not the only factor used when deciding which model are the best suited for refrigeration load forecasting. There should also be a focus on how the model is handling the non-linear effect from the ambient temperature, due to the highly dependency between the ambient temperature and the refrigeration load. In Figure 6.2, the 1-step ahead residuals is plotted against the 1-steps ahead ambient temperature, with a `loess` fitted red line, and corresponding for 36-step horizon, for both model_{diur} and $\text{model}_{sp,on}$.

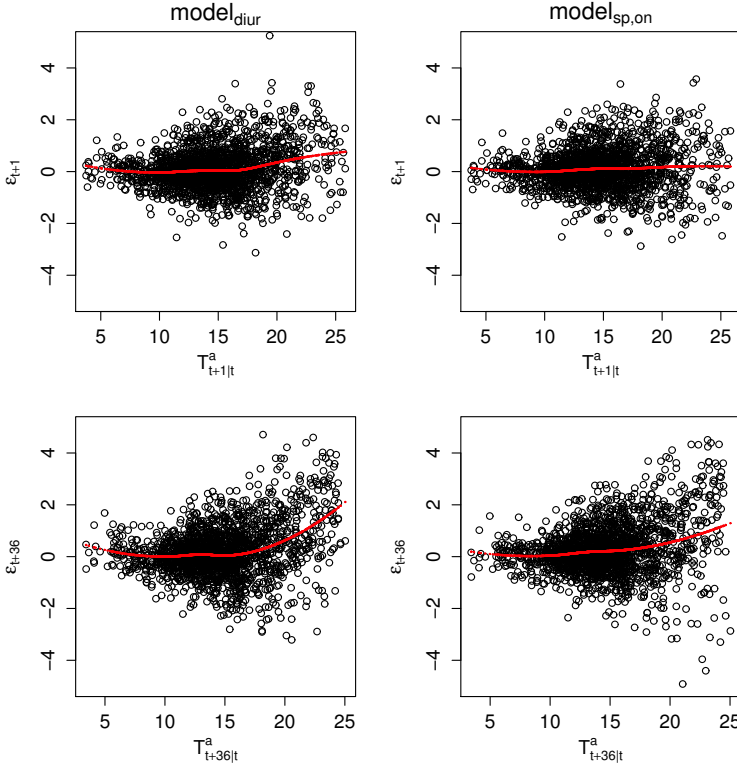


Figure 6.2: Plot of residuals versus ambient temperature for 1-step horizon (top) and 36-step horizon (bottom), to the left $model_{diur}$, to the right $model_{sp,on}$.

Here it is clearly seen that $model_{sp,on}$ is handling the non-linear effect from the ambient temperature better than $model_{diur}$, both models are increasing in the conditional mean of the residuals, but when temperature is above approximately 17 °C in long horizons $model_{diur}$ is more biased than $model_{sp,on}$.

It is found, that the performance increases by modelling the ambient temperature with splines, the downside is that the long horizon forecasts does not have a stable performance, for when the splines is modelled in an on-line setting, which could indicate that the model is over-parametrized. Taking $model_{sp,off}$ into account the splines do have a positive impact on the forecasting of refrigeration load. Something needs to be done with the way it is implemented or handled in the model, to make the performance more stable.

One way to do this, is to implement the splines in the same way as in $model_{sp,off}$,

with the refrigeration load used as input for estimating the spline parameters used with linear regression `lm()`, but instead of using refrigeration load for the same period as forecasting, which is unknown, then it could be tested with refrigeration load from the same period the year before or the same weekday from the week before, still with predicted low-pass filtered ambient temperature used for making the splines. This method for implementing non-linear effect in an off-line setting is a widely used method for Wind Power Forecasting, see Nielsen et al. (2006)

The harmonics made from Fourier series is very useful, because of the daily pattern with the day and night regime and it is easy to implement. The number of harmonics n_{har} could be optimized too, this was done in the report by Bacher et al. (2013) where it was optimized to the highest possible amount of harmonics, $n_{har} = 11$ for each horizon, which indicates that high frequencies are needed in the diurnal curve. When optimizing the parameters with `optim` as mentioned in Section 4.1.5, for the two models with splines input, some computational difficulties occurred in the optimization algorithm, with some matrix operations failing due to singularity, n_{har} was then chosen to 10 for all models, so the models were compared on equal terms, it was only *model_{sp,on}* that needed some small programming fixing as mentioned in the beginning of Section 4.5.1.

The forecasting model developed in this Thesis is able to forecast the aggregated refrigeration load consumption for all coolers and display cabinets in the supermarket Fakta in Otterup, where the coolers and display cabinets are maintained at a fixed temperature with varying external factors, such as ambient temperature. As mentioned in Chapter 1, it is desired to develop a controller that is able to regulate the temperature in the coolers and cabinets, so that more load is consumed when the power is at a low price, i.e. when there is large amount of wind power in the energy system. In that sense, it is useful to know how much load the coolers and cabinets consume for a given temperature, inside the coolers and cabinets.

Having in mind that there is a large probability, that this controlling device is going to be operated by the supermarket it self, it could be an issue that the predicted ambient temperature (NWP's) might not be available or difficult to get hands on, other models without the predicted ambient temperature should then be tested. It could be relevant to test if other local measurements as solar radiation and wind speed, could improve performance without NWP's, maybe using relative humidity in the supermarket as input, could give similar information as the predicted ambient temperature, see Fredslund (2013). This could also lead to a possibility of testing other methods for refrigeration load forecasting, such as a Continuous Time Stochastic Modelling (CTSM-R, see homepage www.ctsm.info). CTSM is a modelling of a dynamical system based on stochastic differential equations, which is determining the states in the system.

If the model is going to be used for one specific cabinet, i.e. a cooling basin with glass, then other conditions should be considered, as the placement of the cabinet in the store, see Fredslund (2013) page 12, which could have more spotlights making the temperature drop faster in the cabinets when it is opened and the defrost cycles, which has a large impact on the daily pattern for the load consumption.

6.1 Future work

Further work and experiments should be done to improve the forecasting model. Below is listed some of which should be tested, or considered in the future work.

- Data from more years should be tested on the models with spline input, to see how it performs, especially the off-line spline model.
- Implementing humidity as input: in the report Fredslund (2013), the refrigeration load is detected to have high non-linear dependency with the relative humidity in the supermarket.
- Coefficients for the low-pass filter could be optimized separately for both regimes, in order to include different dynamical relations in the regimes.
- Modelling the forecast uncertainties: this will give valuable information for the operation of the energy systems, based on fluctuating renewable energy production.
- Include more local observations like solar radiation and wind speed, to determine, if performance improves with use of more local observations
- Develop a model with CTSM.

This is just to mention some of the things that could be tested, to improve the forecasting model, however it is also found that it will be difficult to improve the performance much, due to residuals being very close to white noise.

Further studies could also be, to test the model on other supermarkets, to see if the model is able to adapt to different systems and conditions, or to build a model which enfolds the aspects of many different refrigeration systems and conditions.

Conclusion

A method for forecasting refrigeration load in a Supermarket is developed. It issues refrigeration forecast with hourly values at horizon 1 to 42 hours. Observed refrigeration load and local measured ambient temperature for the period May 1st to August 1st 2012 is used. The method is going to be used as part of the development of a controlling device, which helps making the Supermarket flexible in the energy system.

Initially a simple linear multiplicative seasonal ARIMA model is fitted, with use of only observed refrigeration load. First the data is transformed with the logarithm and differenced twice, with lag 1 and lag 24, then a suitable ARIMA model is identified with use of residual analysis. The most suitable model found was $ARIMA_{(3,1,1) \times (1,1,1)}$.

This model is found inadequate for forecasting refrigeration load, especially for longer horizons, since observations are replaced with predictions, when longer horizons are predicted and the non-linear dependency of the ambient temperature is not included in the model.

An adaptive linear time-series model from the report Bacher et al. (2013) is reconstructed and evaluated for the chosen period. This model is a regime switching model, with the opening and closing hours of the Supermarket as the regimes. The input for this model is a harmonic curve from a Fourier-series and a low-pass filtered predicted ambient temperature, where the model coef-

ficients are fitted in an adaptive recursive least squares with forgetting. The coefficients for the forgetting and low-pass filtering is fitted in an off-line setting by minimizing the $RMSE_k$ for each horizon k . With this model used as foundation, three other adaptive linear time-series models are developed, one with the regime splitting determined by a diurnal curve made from the harmonics, another with the low-pass filtered ambient temperature modelled with splines in an off-line setting, where the ambient temperature is fitted with splines and added to the regressor vector in the RLS algorithm. In the last model the low-pass filtered ambient temperature is modelled with splines in an on-line setting, where the B-splines are added as input to the regressor vector.

The performance of these models are measured by calculating the $RMSE_k$ for each horizon k . $RMSE_k$ for these models have a range of approximately 0.81-0.87 to 1.05-1.12, with the refrigeration load ranging between 2.3 kW and 19.1 kW, it is a relatively small forecasting error. The $RMSE_k$ shows a jump in performance from $k = 24$ to $k = 25$ for all models except $model_{sp,off}$, the jump is caused by the diurnal pattern in the data, the models are using the diurnal curve to compensate for increase in the ambient temperature and are not compensating enough in $k = 25$. For $model_{sp,off}$, the better input from the spline fitted ambient temperature, evens out the behaviour from the diurnal curve. Further investigation should be made for improvement of the diurnal input.

The model with regime from a diurnal curve is better than the basic model from Bacher et al. (2013), with approximately 3 % in average per horizons, but non-linear effect from the ambient temperature is not described sufficiently. Modelling the ambient temperature input with splines improves the handling of the non-linear effect from ambient temperature.

The model with splines in an on-line setting is performing worse than the model with diurnal regime, because of the method for implementing the splines are making the model over-parametrized. The best model for forecasting of refrigeration load is found to be the model with splines created in an off-line setting, but due to use of unknown data some modifications needs to be done before it can be applied in operational environments. One idea for modification of the model with splines in an off-line setting, is to use data from the year before, or the same weekday from the week before.

The estimates for the model coefficients shows great adaptability to changing conditions, but lagging a little on the respond time. From report Bacher et al. (2013), the number of harmonics where optimized to be 11, indicating high frequency is needed, they were not optimized in this Thesis, these models used 10 harmonics, due to some computational difficulties with the splines. The residuals for all models shows close relation to white noise, but also some small bias with the ambient temperature, especially in long horizons. For the models with

splines no bias with the ambient temperature are showing in the residuals for horizon $k = 1$.

It has been found that this method is suitable for forecasting refrigeration load in a Supermarket, improvement is possible and different ideas for improvements is presented. But improvements are difficult to achieve, since the 1-step ahead predictions for model with off-line splines shows residuals close to white noise.

Further work on this model is to fit it with more data and to test if the relative humidity in the Supermarket will have a positive effect on the forecasting performance. Implementing separately low-pass filter coefficients for each regime is also a relatively easy approach for further work.

Other methods besides the adaptive linear time-series model can be tested, i.e. CTSM, which is Continuous Time Stochastic Modelling.

List of Figures

2.1	Top plot is the refrigeration load and bottom plot is the measured ambient temperature of all observations.	6
2.2	Time series plot of the hourly measurements for the selected period, load is the top plot and ambient temperature is the bottom plot.	7
2.3	Time series plot of the hourly measurements for three selected days, for displaying the daily curve.	8
2.4	Scatterplots of the observed ambient temperature versus NWP, to the left is with the NWPs in UTC-time and observed in local time, to the right the NWPs are lagged to local time.	9
2.5	Scatterplots of the observed temperature versus the NWP for 1-step ahead (left plot) and 36-step ahead (right plot), including a line with the slope of 1 and intercept 0.	10
2.6	Scatterplot of ambient temperature as a function of predicted ambient temperature 1-step ahead to the left and 36-step ahead to the right, inclusive the loess fitted values, with different spans.	11
2.7	$RMSE_k$ for the difference between the loess fitted ambient temperature and predicted temperature from period May 1 st to August 1 st 2012, for horizon 1 to 42.	12

2.8	RMSE _k for the difference between the loess fitted ambient temperature and predicted temperature from the whole period, for horizon 1 to 42.	13
2.9	Time series plots of the load, before gaps are replaced (top) and after gaps are replaced (bottom).	14
2.10	Ambient temperature versus load, for opening hours (left) and closing hours (right), with a loess fit curve.	15
3.1	The model building procedure.	19
3.2	Box-Cox transformation patterns.	21
3.3	Range-mean plot, with 24 groups.	24
3.4	The upper figure is with the originally observed hourly load consumption and the lower figure are the logarithm of the hourly load consumption.	25
3.5	The upper figure shows the ACF for 72 lags and the lower figure shows for the entire series.	25
3.6	Plots of a sub-part of the differenced series and corresponding ACF plot.	26
3.7	Residuals, cumulative periodogram, ACF and PACF plot for $ARIMA_{(0,1,1) \times (0,1,1)_{24}}$	28
3.8	Residuals, cumulative periodogram, ACF and PACF for $ARIMA_{(0,1,1) \times (1,1,1)_{24}}$	30
3.9	Residuals, cumulative periodogram, ACF and PACF for $ARIMA_{(6,1,1) \times (1,1,1)_{24}}$	32
3.10	Residuals, cumulative periodogram, ACF and PACF for $ARIMA_{(3,1,1) \times (1,1,1)_{24}}$	34
3.11	The predicted refrigeration load and the observed refrigeration load.	35
4.1	An example of a square wave Fourier series made from $\frac{4}{\pi} \sum_{n=1,3,5..}^{11} \frac{1}{n} \sin(\frac{t_{load} n \pi}{12})$	40
4.2	Example of a quadratic B-spline with a triple knot.	42

-
- 4.3 Spline function with three B-splines, from 1000 simulated values from the uniform distribution with a random spread. 43
- 4.4 The fitted model parameters as a function of horizon k for $model_{basic}$. 46
- 4.5 Scatter plots of the load versus the ambient temperature, showing the splitting with opening and closing hours. The black points is the opening regime, the red points indicates the closing regime. In the left plot the closing regime is plotted on top of the opening regime and vice versa in the right plot. 47
- 4.6 $RMSE_k$ for each horizon $k = 1$ to $k = 42$ for $model_{basic}$ 48
- 4.7 Residuals from 1-step ahead predictions (to the left) and 36-step ahead predictions (to the right) for $model_{basic}$ 49
- 4.8 First plot shows the 1-step ahead forecast and the refrigeration load for the 21st of May and 22nd of May 2012, bottom plot is the corresponding residuals, for $model_{basic}$ 50
- 4.9 Residuals from $model_{basic}$ for 1-step ahead predictions (to the left) and 36-step ahead predictions (to the right) without the two excluded residuals. 51
- 4.10 The ACF, histogram and QQ-normal plot for the 1-step ahead residuals, for $model_{basic}$ 52
- 4.11 First plot is the forecast versus the refrigeration load, next plot is the observed ambient temperature and the last plots is the fitted coefficients for the ambient temperature input, first the intercept and slope for the open regime and the corresponding plots for closing regime, for $model_{basic}$ 53
- 4.12 1-step and 36-step ahead residuals versus the predicted ambient temperature used as input, with smoothed local regression estimates as red lines, for $model_{basic}$ 54
- 4.13 Scatter plots of the load versus the ambient, showing the splitting with the diurnal curve. The black points is the positive values indicating day regime, the negative values are the red points indicating the night regime. In the left plot the night regime is plotted in top of the day regime and vice versa in the right plot. 56
- 4.14 The fitted model parameters as a function of horizon k , for $model_{diur}$. 57

4.15	RMSE _k for each horizon $k = 1$ to $k = 42$, for $model_{diur}$	58
4.16	Residuals from $model_{diur}$ for, 1-step ahead predictions (to the left) and 36-step ahead predictions (to the right).	59
4.17	The ACF, histogram and QQ-normal plot for the 1-step ahead residuals, for $model_{diur}$	60
4.18	First the forecast versus the refrigeration load, next plot is the observed ambient temperature and the last plots is the fitted coefficients for the ambient temperature input, first the intercept and slope for the day regime and the corresponding plots for night regime, for $model_{diur}$	61
4.19	1-step and 36-step ahead residuals versus the predicted ambient temperature used as input, with smoothed local regression estimates as red lines, for $model_{diur}$	62
4.20	Examples of a good choice of knots (to the left) and a bad choice of knots (to the right).	65
4.21	The B-splines used as input for 1-step prediction plotted against the low-pass filtered ambient temperature input, divided in the day and night regime, for $model_{sp,off}$	66
4.22	The fitted model parameters as a function of horizon k , for $model_{sp,off}$	67
4.23	The RMSE _k for each horizon k , for $model_{sp,off}$	68
4.24	The residuals for horizon $k = 1$ (to the left) and $k = 36$ (to the right), for $model_{sp,off}$	69
4.25	The ACF, histogram and QQ-normal plot for the 1-step ahead residuals, for $model_{sp,off}$	69
4.26	First plot shows the forecast versus the refrigeration load, next plot is the observed ambient temperature and the last plots is the fitted coefficients for the ambient temperature input, both the intercept and the slope for the day and night regimes, for $model_{sp,off}$	71
4.27	1-step prediction errors and 36-step prediction errors with loess fitted red lines, for $model_{sp,off}$	72

4.28	The B-splines used as input for 1-step prediction plotted against the low-pass filtered ambient temperature input, divided in the day and night regime, for $model_{sp,on}$	73
4.29	The fitted model parameters as a function of horizon k , for $model_{sp,on}$	74
4.30	The $RMSE_k$ for each horizon k , for $model_{sp,on}$	75
4.31	The residuals for horizon $k = 1$ (to the left) and $k = 36$ (to the right), for $model_{sp,on}$	76
4.32	The ACF, histogram and QQ-normal plot for the 1-step ahead residuals, for $model_{sp,on}$	76
4.33	Plots of each coefficients for the B-splines, in the day and night regime respectively, the first in each column, the B-spline B_1 day and B_1 night corresponds to the B-spline β_i for the intercept, together with the B-spline inputs, for $model_{sp,on}$	77
4.34	1-step residuals and 36-step residuals versus the ambient temperature input with loess fitted red lines, for $model_{sp,on}$	78
5.1	Plot of the $RMSE_k$ from each model, for horizon $\{k = 1, \dots, 42\}$	80
6.1	Plot of the observed and the predicted refrigeration load, for $k = 24$ and $k = 25$, together with the corresponding residuals and diurnal input, in period 19 th to 27 th of May for $model_{diur}$	84
6.2	Plot of residuals versus ambient temperature for 1-step horizon (top) and 36-step horizon (bottom), to the left $model_{diur}$, to the right $model_{sp,on}$	86

List of Tables

2.1	List of low temperature cabinets.	6
2.2	List of medium temperature cabinets.	6
3.1	Parameter estimates and standard errors for model $ARIMA_{(0,1,1)\times(0,1,1)_{24}}$	27
3.2	Parameter estimates and standard errors, for model $ARIMA_{(0,1,1)\times(1,1,1)_{24}}$	29
3.3	Parameter estimates and standard errors, for model $ARIMA_{(6,1,1)\times(1,1,1)_{24}}$	31
3.4	Results from the test for lower order model, with parameters from $ARIMA_{(6,1,1)\times(1,1,1)}$	33
3.5	Parameter estimates, standard deviation and test statistics for model $ARIMA_{(3,1,1)\times(1,1,1)_{24}}$	33
3.6	Predicted load in kW, for horizon 1 to 48.	35
5.1	The $RMSE_1$ per model.	79

Bibliography

- P. Bacher, Henrik Madsen, and Henrik Nielsen. Load forecasting for households. Technical report, DTU Informatics, Grundfos A/S, ENFOR A/S, 2012.
- Peder Bacher, Henrik Madsen, and Henrik Nielsen. Online short-term solar power forecasting. *Solar Energy*, 83:1772–1783, 2009.
- Peder Bacher, Henrik Madsen, and Henrik Nielsen. Load forecasting for supermarket refrigeration. Technical report, DTU Compute & ENFOR A/S, 2013.
- James E. Braun and Nitin Chaturvedi. An inverse gray-box model for transient building load prediction. *HVAC&R Research*, 2002.
- D Datta, SA Tassou, and D Marriott. Application of neural networks for the prediction of the energy consumption in a supermarket. *Citeseer*.
- Carl de Boor. *A Practical Guide to Splines*. Springer, 2001.
- DMI. Dmi-hir1am-s05. URL http://www.dmi.dk/eng/index/research_and_development/dmi-hir1am-2009.htm.
- Ioan Felea, Florin Dan, and Simona Dzitac. Consumers load profile classification correlated to the electric energy forecast. Technical report, University of Oradea, 01 2012.
- Kristian Fredslund. Load profiles for supermarket refrigeration. Technical report, IPU, 2013.
- M.J. Jiménez, Henrik Madsen, and K.K. Andersen. Identification of the main thermal characteristics of building components using matlab. *Elsevier Ltd.*, 2008.

- Henrik Madsen. *Time Series Analysis*. Chapman & Hall/CRC, 2008.
- Henrik Madsen and J. Holst. Estimation of continuous-time models for the heat dynamics of a building. *Elsevier Ltd.*, 1995.
- Robert F. Nau. Identifying the numbers of ar or ma terms. URL <http://people.duke.edu/~rnau/411arim3.htm>.
- H.A. Nielsen and H. Madsen. Predicting the heat consumption in district heating systems using meteorological forecasts. Technical report, DTU IMM, 2000.
- Hans Bruun Nielsen. Cubic splines. Technical report, IMM, 1998.
- Henrik Nielsen and Henrik Madsen. Modelling the heat consumption in district heating system using a grey-box approach. *Energy and Buildings*, 38:63–71, 2006.
- T.S. Nielsen, H. Madsen, H.A. Nielsen, P.Pinson, G. Kariniotakis, N. Siebert, I. Marti, M. Lange, U. Focken, L. von Bremen, P. Louka, G. Kallos, and G. Galanis. Short-term wind power forecasting using advanced statistical methods. In *Proceedings of The European Wind Energy Conference, EWEC 2006*, 2006.
- www.ctsm.info. Continuous time stochastic modelling.